SYSTEMATICS

Chattonella verruculosa and Related Species from Japan, Europe (North Sea) and U.S. Coastal Waters: Cases of Mistaken Identity?

Carmelo R. Tomas[1], Chitari Ono[2], Sadaaki Yoshimatsu[2], and Jeanette Göbel[3]
[1]*University of North Carolina at Wilmington, Center for Marine Science, 5600 Marvin Moss Lane, Wilmington, NC 28409, USA;*
[2]*Akashiwo Research Institute of Kagawa Prefecture, 75-5 Higasi-machi, Takamatsu, Kagawa 761-0111, Japan;*
[3]*Landesamt fuer Natur und Umwelt, Hamburger Chaussee 25, D 24220 Flintbek, Germany*

Abstract

Three clonal cultures referred to as *Chattonella verruculosa* were studied as to their morphology, pigment content and capacity to kill fish using a standard fish bioassay. One clone, *C. verruculosa* (CVJapan), was isolated from a fish kill in an aquaculture facility in Japan. A second, *C.* aff. *verruculosa* (CVNS), was isolated from the North Sea and is similar to the species that formed blooms in Norway. The third, *C.* cf. *verruculosa* (CVDel), was isolated from a bloom in Rehoboth Bay, Delaware, where nearly 2×10^6 *Brevoortia tyrannus* (Menhaden) were found dead. Morphologically, all three species were similar, having spherical, pyriform or irregular cells. Two (CVJapan and CVNS) formed benthic multiflagellated irregular masses of cells. Of the three, CVDel was green to green-yellow in pigmentation while the others were golden-brown. Pigment composition (HPLC) was similar for the CVJapan and CVSN, but that of CVDel was markedly different. All cells were found to cause fish mortality when examined using the *Gambusia affinis* fish bioassay. It is more likely that CV Japan and CVNS are the same or similar species and that CVDel, from Delaware, is a morphologically related but totally different species.

Introduction

Two species of the Raphidophyceae genus *Chattonella* (*C. antiqua* and *C. marina*) are reported to be the causative agents of fish mortalities in Japan (Okaichi, 1983) and Australia (Hallegraeff *et al.,* 1998). Both species are known to produce several potent brevetoxin-like compounds (Onoue and Nozawa, 1989, Kahn *et al.,* 1995, 1999, Ahmed *et al.,* 1995) as well as the reactive oxygen species (ROS) as OH^{-1}, H_2O_2 and O_2^- (Yang *et al.,* 1995, Kim *et al.,* 1999, Skeen, this Proceedings), which may act alone or in combination with fatty acids (Marshall, this Proceedings) to cause fish kills. The species *C. verruculosa* (Hara *et al.,* 1994) was also reported (Yamamoto and Tanaka, 1990; Baba *et al.,* 1995) to cause fish mortality in Japan in aquaculture and natural waters. More recently (1998–2000), a similar species (*C.* aff. *verruculosa*) reported from the Norwegian and Danish coasts caused mortalities of pen-reared salmon, but wild fish were not affected (Backe-Hansen, 2000). This species formed blooms in the North Sea (2000–01) (Lu and Göbel, 2001) and Norwegian coastal waters (Algen Post), with losses in excess of 800 tons of salmon. During the summer of 2000, over 2 million menhaden (*Brevoortia tyrannus*) perished in Rehoboth Bay, Delaware, (USA) during a bloom that exceeded 10^7 cells · L^{-1} of *C.* cf. *verruculosa* (Bourdelais *et al.,* 2002). Water sampled from that bloom contained three brevetoxin fractions (PbTx-2, -3, -9) confirmed by multiple analyses using HPLC, brevetoxin specific ELISA (Naar *et al.,* 2002), NMR spectrometry and mass spectroscopy. Of the *Chattonella* species, *C. verruculosa* is the least understood. This work offers a preliminary comparison of cultures and natural material of *C. verruculosa* (either as *C. verruculosa, C.* aff. *verruculosa*, or *C.* cf. *verruculosa*) in an effort to better define the identity of these fish killers and to indicate their potential roles in the loss of fishery resources.

Materials and Methods

Cultures of *C. verruculosa* studied were obtained from the Akashiwo Research Institute (CVJapan, Takamatsu, Japan).*C.* aff. *verruculosa* were obtained from the North Sea by J. Göbel (CVNS, LANU Institute, Germany) and isolated from 2000–01 blooms in Rehoboth Bay, Delaware (CVDel, Tomas, CMS/UNCW). Cultures were grown in erdschreiber and F/2 medium at 20°C, 12:12 LD of cool white fluorescent light (100 μE m^{-2} s^{-1}). All cultures were observed live using a Nikon Diaphot Inverted microscope equipped with an optronix digital camera or a Zeiss Axioscope 2IE with a Zeiss Axiocam and imaging software. Pigment profiles were conducted from methanol extractions (Wright *et al.,* 1991) using a Shimadzu SPD10 AUV HPLC with diode array detector from cultures filtered on a GFF glass fiber filter that had been frozen at –80°. Toxicity was tested using the *Gambusia affinis* standard fish bioassay. Mortality of fish that occurred within 2–4 hours of exposure was considered positive results indicating ichthyotoxicity.

Results and Discussion

Observations of the general morphology of the CVJapan and CVNS (North Sea) demonstrated a high degree of variability (Fig.1). The spherical form described by Hara *et al.* (1994) with two flagella, a short carried forward and another slightly longer trailing, emerging from the anterior of the cell, was not the predominant form in either of the cultures. More common were "tear drop" pyriform-shaped cells with two flagella emerging from a subapical groove (Fig. 1A–C). All cells had pyriform moderately motile cells with "lumpy" or verruculose surfaces (Fig. 1A,B).

In addition to pyriform cells, a number of elongated, irregular to broadly oval cells (Fig. 1C) were seen in both the Japan and North Sea clones. While the spherical cells were less common (Fig. 1D), they were abundant towards the bot-

Steidinger, K. A., J. H. Landsberg, C. R. Tomas, and G. A. Vargo (Eds.). 2004. Harmful Algae 2002. Florida Fish and Wildlife Conservation Commission, Florida Institute of Oceanography, and Intergovernmental Oceanographic Commission of UNESCO.

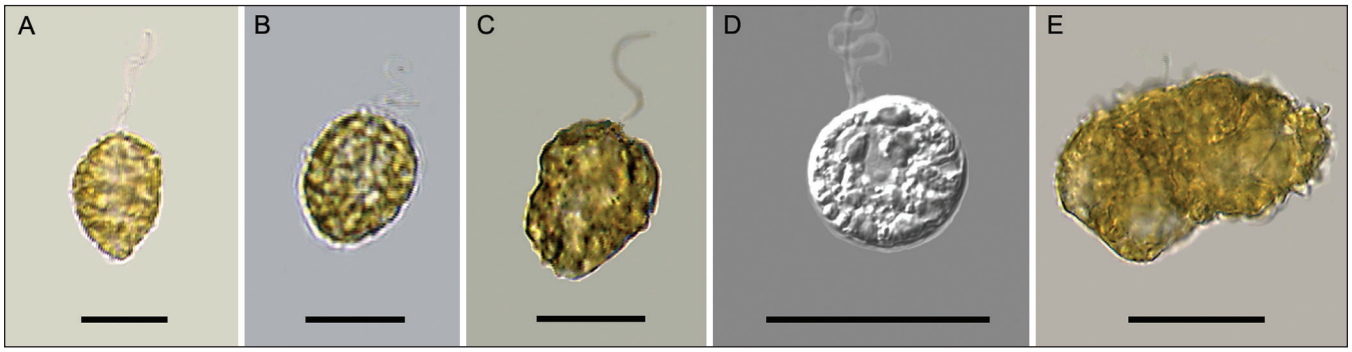

Figure 1 *Chattonella verruculosa* from the North Sea and Japan. **A** CVNS; **B** CVJapan pyriform cells; **C** oval CVJapan cells; **D** spherical CVJapan; **E** multiflagellated mass from CVJapan.

tom of the culture flasks, suggesting they might be less motile than other cells. Another feature common in both cultures was the formation of multiflagellated masses (Fig.1E) that were weakly or totally non-motile and more common in older cultures. The exact nature of these masses is unknown but nuclear staining with DAPI did indicate that they had multiple nuclei, suggesting "cleavage monsters" similar to those observed in *Euglena deses* (Leedale 1967). With respect to other features, cells of both CVJapan and CVNS clones were largely pigmented as golden-brown. In comparison, cells of CVDel also had varying morphologies as the other clones did but appeared to have green plastids and often were seen as elongated cells with blunt anterior, lacking color, (Fig. 2A.) and with two flagella emerging from a subapical groove. Spherical and oval cells with two emergent flagella (Fig. 2B,C) and with similar pigmentation were also observed. Single, spherical non-motile cells (Fig. 2 D) were also found in the CVDel cultures. When motile cells were preserved with gluteraldehyde (Fig. 2F), they became undistinguishable spherical masses with a clear area around them suggesting the excretion of a mucoid-like compound. Unlike CVJapan and CVNS, multicellular masses at the bottom of each culture flasks were never observed in the CVDel clones.

The 18S ribosomal DNA data (Oldach *et al.,* this Proceedings) from both CVJapan and CVNS failed to link the two species and grouped them separately. In contrast, the Delaware clone was grouped with the Raphidophytes but not with CVNS. The pigment data (Table 1) shows a similarity of the Japan and North Sea clones and contrasts that of the Delaware clone. Clone CVDel totally lacks Chl_b and Chl_{c3} and was lower in fucoxanthin that the other clones. The absence of 19′-butanoyloxyfucoxanthin, common in the CVJapan and CVNS clones, was not found in the Delaware clone. Other differences in pigments observed for CVDel were higher values in the accessory pigments violaxanthin, diadinoxanthin, antheroxanthin, lutein and zeaxanthin. The lack of fucoxanthin and elevated levels of diadinoxanthin and antheroxanthin, as well as an elevated level of chl *a* (>70% relative CVDel to ~45–60% for other clones), could explain the strongly green pigmentation absent in the two other clones.

A suggestion that CVDel may be a *Eutreptiella* was not supported by the pigment and 18S sequence data. The CVDel clone was distinctly different from the two other clones, and while it has some affinities with the Raphidophyceae, further detailed studies of pigments and morphology are needed. Green Raphidophytes are not uncommon. Both *Vacuolaria* and *Gonystomum* are green in appearance. Most recently, green blooms of *Heterosigma akashiwo* were observed in coastal waters with HPLC pigments profiles consistent with *H. akashiwo* (Tomas, unpublished data). Clearly, further comparison of CVDel with species like *Vacuolaria* and *Gonystomum* are needed prior to further conclusions about the placement of this species.

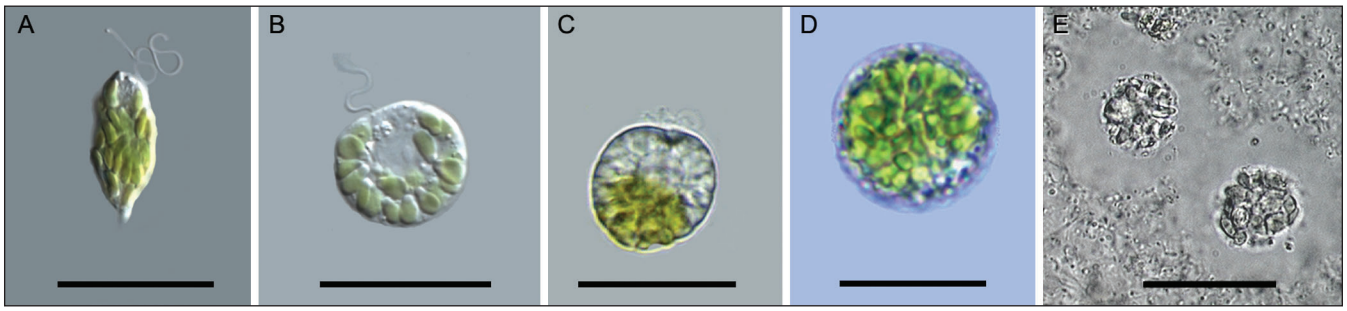

Figure 2 *C. verruculosa*-like cells from Delaware bloom. **A** Pyriform cell; **B** and **C** spherical and oval cells with anterior region lacking plastids; **D** non-motile spherical cells (Cysts?); **E** gluteraldehyde-fixed cells.

Table 1 Chlorophyll-corrected HPLC pigments for the three *C. verruculosa*-like cultures.

Pigments	Cv. Japan	Cv. North Sea	Cv. Delaware
Chl *a*	1.0000	1.0000	1.0000
Chl c^1+c^2	0.3588	0.3542	0.0937
Chl c^3	0.1120	0.0919	0.0000
19' butanoyl	0.1215	0.1671	0.0000
Fucoxanthin	0.3707	0.3675	0.0810
Violaxanthin	0.0028	0.0014	0.0048
Diadinoxanthin	0.1657	0.0232	0.1612
Antheraxanthin	0.0167	0.0000	0.1037
Lutein	0.0013	0.0003	0.0241
Zeaxanthin	0.0080	0.0021	0.0369

All three clones were found to be toxic to *Gambusia affinis* in the standard fish bioassay. Levels of 10^6 cells · L^{-1} were required to cause mortality of fish exposed for 2–4 hours. The toxicity was approximately equivalent for each clone based on cell densities. The exact nature of the toxin was not determined, however, and extracts from each culture showed similarities to other polyether toxins known from other Raphidophyceae (Bridgers *et al.,* this Proceedings).

The morphological observations, 18S ribosomal DNA sequences and pigment data taken together clearly separate the three clones into different groups. Clones of CVJapan and CVNS appear to be identical or very similar, suggesting a similar origin. The sequence data, pigments and morphology also support the contention by Honda (personal communication) that *C. verruculosa* is not a Raphidophyte, but based on 18S sequences and electron microscopic evidence, that it belongs to the Dictyocophyceae and not the Raphidophyceae. The CVDel was definitely separated from the other *Chattonella* clones but more closely aligned with the Raphidophyceae. The pigment data indicate that this species does not belong to this class and further details are needed for accurate placement of it into a proper taxon. Thus surprisingly, all three cases of clones identified as *Chattonella verruculosa* are, in fact, a case of mistaken identity.

Acknowledgements

We wish to thank Dr. D. Honda for his information regarding the unpublished 18S and EM data on *C. verruculosa* from Japan. We are grateful to Dr. Gary Kirkpatrick of Mote Marine Laboratory for running the HPLC pigment spectra and Dr. Olga Mangoni for confirming pigment composition. This project was supported in part by the grant NCWRRI NCSU 2001-0095-02 awarded to C. Tomas.

References

S. Ahmed, S. Kahn, O. Arakawa and Y. Onoue, Biochim. Biophys. Acta 1234, 509–512 (1995).

T. Baba, K. Momoyama and M. Hiraoka, Bull. Yamaguchi Pref. Naikai Fish. Exp. Stn. 24, 121–122 (1995).

P. Backe-Hansen, E. Dahl and D. S. Danielssen, in: Harmful Algal Blooms, G. Hallegraeff (ed.), 87 (2000).

A. Bourdelais, C. R. Tomas, J. Naar, J. Kubanek and D.G. Baden, Environ. Health Perspect. 110 (5), 465–470 (2002).

G. M. Hallegraeff, B. L. Munday, D. G. Baden and P. L. Whitney, in: Harmful Algae, B. Reguera, J. Blanco, M. L. Fernández and T. Wyatt, eds. (Xunta de Galicia and IOC, UNESCO, Paris), pp. 93–96 (1998).

Y. Hara, K. Doi, and M. Chihara, Jpn. J. Phycol. 42, 407–420 (1994).

S. Kahn, M.S. Ahmed, O. Arakawa and Y. Onoue, Isr. J. Aquacult. 47(3–4), 137–141 (1995).

S. Kahn, M.M. Haque, O. Arakawa and Y. Onoue, Bangladesh J. Fish. 19(1–2), 71–77 (1996).

C.S. Kim, S.G. Lee, C.K. Lee, H.G. Kim and J. Jung. J. Plankton Res. 21(11), 2105–2115. (1999).

G. F. Leedale, Euglenoid Flagellates, Prentis Hall, 242 p. (1967).

D. Lu and J. Göbel, HAMM 2001 Web Page (2001).

J. Naar, A. Bourdelais, C. Tomas, J. Jubanek, P.L. Whitney, L. Flewelling, K. Steidinger and J. Landcaster. Environ. Health Perspect. 110(2), 179–184 (2002).

T. Okaichi, J. Oceanogr. Soc. Jpn. 39, 267–278 (1983).

Y. Onoue and K. Nozawa, in: Red Tides: Biology, Environmental Science and Toxicology, T. Okaichi, D.M. Anderson and T. Nemoto, eds. (Elsevier, Amsterdam), pp. 371–374 (1989).

S. W. Wright, S. Jeffrey, R. Mantoura, C. Llewellyn, C. Bjornland and D. Repeta, Mar. Ecol. Prog. Ser. 77, 183–196 (1991).

C.Z.Yang, L. J. Albright and A. N. Yousif. Dis. Aquat. Org. 23, 101–108. (1995).

C. Yamamoto, and Y. Tanaka, Bull. Fukuoka Fish. Exp. Stn. 16, 43–44 (1990).

Dinoflagellates Come from Outer Space, but Haptophytes and Diatoms Do Not

Uwe John[1], Thomas Mock[1], Klaus Valentin[1], Allan D. Cembella[2], and Linda K. Medlin[1]
[1]*Alfred-Wegener-Institut, Postfach 120161, D-27570 Bremerhaven, Germany;*
[2]*Institute for Marine Biosciences, National Research Council (Canada), 1411 Oxford St., Halifax, Nova Scotia, Canada B3H 3Z1*

Abstract

Normalized cDNA libraries were generated for a dinoflagellate (*Alexandrium ostenfeldii*) and a haptophyte (*Chrysochromulina polylepis*), both photosynthetic species capable of forming toxic blooms. Partial sequences were obtained from 2500 clones from each library. After annotation, these represented about 1400 unique sequences for each species. Several genes putatively related to toxin synthesis were detected. Yet only 9% of the total sequences were homologues to known genes for *A. ostenfeldii,* whereas the corresponding number for *C. polylepis* was 32%. A cDNA library for the psychrophilic diatom *Fragilariopsis cylindrus* was also established after cold-shock treatment. From this library, 350 clones were partially sequenced and 40% were identified by BLAST search. In summary, the percentage of identifiable genes in the dinoflagellate was substantially lower than in other protists examined. These data provide preliminary indications that dinoflagellates possess a radically different genome from other "algal protists" and thus their uniqueness makes them interesting candidates for genomics research.

Introduction

As members of the phytoplankton, diatoms and free-living dinoflagellates are often the dominant eukaryotic groups contributing to plankton biomass and primary production in both coastal and oceanic waters. Yet unlike the diatoms and other phytoplankton, dinoflagellates have long been considered as belonging to both the botanical and zoological realm, because this group comprises many heterotrophic and parasitic forms. In fact, the dinoflagellates have more apparent affinities with ciliates and certain amoebae than with classic microalgal groups, posing a problem in the construction of an explicit phylogeny for the lower eukaryotes (Taylor, 1980). Although a few genes (18S and 28S rDNA, in particular) are frequently sequenced for phylogenetic reconstruction, there is little genomic information on the major groups of eukaryotic microalgae. Even less genomic data is available on gene expression related to primary and intermediary metabolism, biosynthesis of secondary metabolites, including toxins, and the molecular ecology of adaptation to ecological niches. One attempt to resolve these unknowns is to apply the technologies for mass sequencing of genomic DNA of key microalgal species. Such species may include important primary producers, *e.g.,* spring-bloom diatoms; those involved in harmful algal blooms (HABs), *e.g.,* certain dinoflagellates, haptophytes, and raphidophytes; or psychrophiles, *e.g.,* sea-ice microalgae. Although at present it is not practical to completely sequence the genomes of all key species, much information can be gained from random sequencing of cDNA libraries, *i.e.,* by generating expressed sequence tag (EST) libraries. Such libraries are constructed by extracting the messenger RNA, which represents the transcripts of all genes being expressed at a given time. These mRNAs are converted to DNA by reverse transcriptase, cloned, and randomly sequenced. Each clone essentially represents a single gene. In this study, we compared the percentage of identifiable genes from cDNA libraries obtained from the diatom *Fragilariopsis cylindrus,* the toxic dinoflagellate *Alexandrium ostenfeldii,* and the toxic haptophyte *Chrysochromulina polylepis.*

Materials and Methods

Culture and Harvesting of Algae Unialgal cultures were grown in 10-L glass flasks on 14:10 h light:dark cycle in a controlled growth chamber. *Chrysochromulina polylepis* B1511 from Oslo Fjord, Norway, was grown in IMR/2 growth medium (Eppley *et al.,* 1967), supplemented with 10 nM selenite; *Alexandrium ostenfeldii* AOSH1 from Ship Harbour, Nova Scotia, Canada in K medium (Keller *et al.,* 1987); and *Fragilariopsis cylindrus,* isolated from Antarctic sea-ice in the eastern Weddell Sea, was grown in f/2 medium (Guillard and Ryther, 1962). *Fragilariopsis cylindrus* was grown at 5°C at a photon flux density of 35 µmol m^{-2} s^{-1}. The other species were maintained at 15°C, at a photon flux density of 45 µmol m^{-2} s^{-1} for *C. polylepis,* and 90 µmol m^{-2} s^{-1} for *A. ostenfeldii.* All cultures were harvested in the middle of exponential growth by continuous flow centrifugation.

Isolation of mRNA Total RNA of *C. polylepis* and *F. cylindrus* was isolated with an RNeasy Plant Mini Kit (Qiagen, Hilden, Germany). For *F. cylindrus,* mRNA was isolated from ca. 100 µg total RNA with an Oligotex mRNA Midi-Kit (Qiagen, Hilden, Germany.) Total RNA of *A. ostenfeldii* was extracted with peqGOLD RNApure (PEQLAB Biotechnology, Erlangen, Germany) and cleaned with peqGOLD Optipure following manufacturer's instructions.

cDNA Library Construction and Sequence Analysis Normalized cDNA libraries of *C. polylepis* and *A. ostenfeldii* were constructed in cooperation with BASF Plant Science (Ludwigshafen, Germany) and prepared by Vertis Biotechnologie AG (Freising, Germany). The cDNAs were synthesised from 2.4 µg total RNA and directionally cloned into Not I/Asc I-sites of a plasmid vector pFDX3840 (sup-

Steidinger, K. A., J. H. Landsberg, C. R. Tomas, and G. A. Vargo (Eds.). 2004. Harmful Algae 2002. Florida Fish and Wildlife Conservation Commission, Florida Institute of Oceanography, and Intergovernmental Oceanographic Commission of UNESCO.

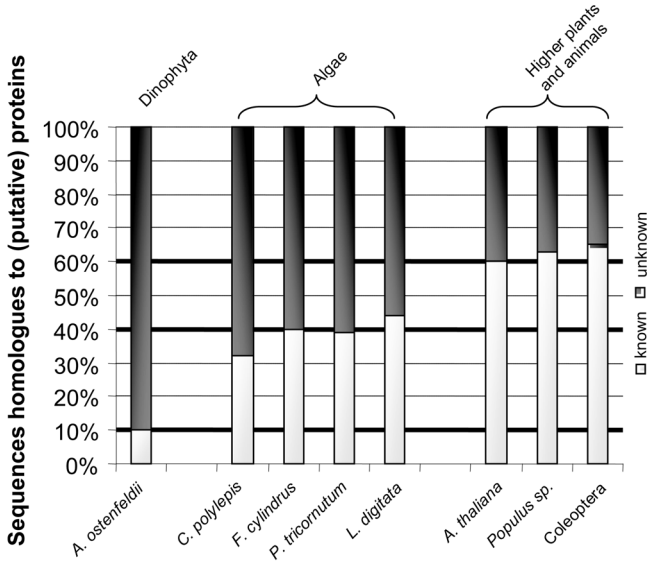

Figure 1 Comparison of ESTs of several species of different systematic groups. Dark bar shows percentage of unknown sequences; light bar indicates percentage of ESTs that show homology to proteins or putative proteins.

plied by Prof. Dr. Ralf Reski, Freiburg). The cDNA libraries were normalised to reduce redundant DNA, ideally leaving only a single copy of each expressed gene to be cloned and sequenced. Normalisation of the cDNA was performed according to Ko (1990) with several modifications. The cDNA library of *F. cylindrus* was synthesised with approximately 800 ng mRNA using a SMART™ cDNA Library Construction Kit (Clontech) following the manufacturer's instructions. White plaques were used for large-scale PCR analysis with 5´and 3´ λTripEx LD-Insert Screening Amplimers. Approximately 350 clones larger than 564 bp were chosen for sequencing analysis. From each normalised cDNA library of *C. polylepis* and *A. ostenfeldii,* 2500 clones were sequenced from the 5' end. The inserts from *F. cylindrus* were also sequenced from the 5' end using λTripEx2 Sequencing Primer. On average, 500 bp were determined. Sequences were compared to detect overlapping clones. All contiguous segments were compared to gene libraries (*e.g.,* GenBank) by BLAST searches and all possible reading frames were analysed.

Results

Expressed Sequence Tag (EST) Libraries (Fig. 1) After annotation, the partial sequences of 2,500 clones from normalised cDNA libraries represented 1,443 unique sequences for *C. polylepis* and 1,416 for *A. ostenfeldii.* In the case of *C. polylepis,* 466 (32%) sequences were homologous to known proteins and 617 (46%) to sequences in EST databases. However, only 120 (9%) of the sequences of *A. ostenfeldii* were homologous to known proteins, whereas 541 (38%) showed similarity to EST sequences. Eight putative polyketide synthase (PKS) genes were identified for *C. polylepis,* and two putative PKS genes were found for *A. ostenfeldii.* The phage cDNA library of the diatom *F. cylindrus* comprised approximately 1.5 Mio recombinant clones per milliliter, and thus likely covered the expressed genome at this time point. Of the 186 EST contigs, 72 (40%) showed homology to known proteins or hypothetical conserved open reading frames (ORFs).

Discussion

The percentage of identifiable genes in the dinoflagellate *Alexandrium ostenfeldii* was dramatically lower than for other protistan algae, indicating that dinoflagellates possess a highly unusual genome. The unique characteristics of dinoflagellates with respect to ultrastructure (extra-nuclear spindle, permanently condensed chromatin, etc.), ploidy (typically *n* in the vegative stage), high amount of nuclear DNA, general absence of histones and nucleosomes, and unusual mitosis, meiosis and life history, support the conclusion that much of the DNA may be non-coding and structural, perhaps subjected to a high degree of redundancy. The low degree of similarity of cDNAs in the dinoflagellate to known sequences further suggests that metabolic pathways may also be rather divergent. A comparative study of ESTs in the toxigeneic dinoflagellate, *Karenia brevis,* did show a higher degree of homology to known genes (32%) in other organisms than we found for *A. ostenfeldii* (Lidie *et al.,* 2003). The abundancy expressed genes were primarily related to general metabolism, signal transduction and transcription/translation. The phylogenetic relationship between dinoflagellates, particularly parasitic and heterotrophic species, and apicomplexans has been recognized, although recent molecular studies on the fish-killing dinoflagellate *Pfiesteria piscicida* and other *Pfiesteria*-like dinoflagellates showed that these dinoflagellates form a distinct group and are not that clearly related to the apicomplexa (Litaker *et al.,* 1999). While we do not literally mean to imply that dinoflagellates are extraterrestrial in origin (from "outer space"), our data suggest that a genomic project on dinoflagellates would likely identify interesting and new, perhaps even highly abnormal, genes.

The percentage of identifiable genes in the two chromophytic microalgae examined in this study was similar and approximately two-thirds of that of higher plants, such as *Arabidopsis thaliana* (Meinke *et al.,* 1998) and two woody *Populus* species (Sterky *et al.,* 1998), or animals such as coleopteran insects (Theodorides *et al.,* 2002). Degrees of similarity were in the same range as for two other chromophytes, *e.g., Laminaria digitata* (Phaeophyta), Crepineau *et al.,* 2000; and *Phaeodactylum tricornutum* (Bacillariophyta), Scala *et al.,* 2002. Chromophytic algae contain, however, a higher percentage of unknown genes than higher plants (Meinke *et al.,* 1998). This is not surprising because heterokonts and haptophytes represent evolutionary lineages that separated from other eukaryotic lineages around 1200 million years ago (Medlin *et al.,* 1997), and molecular data on chromophytes are much less studied than for higher plants.

Despite the fact that only a limited number of ESTs were sequenced for the toxigenic species, several significant genes were detected. In both toxic species, *A. ostenfeldii* and *C. polylepis,* a number of genes encoding polyketide synthases (PKS) was found. These genes are known to be involved in the biosynthesis of certain potent polyketide phycotoxins, including spirolides, diarrhetic shellfish poisoning toxins, and brevetoxins (Wright and Cembella, 1998). Their detection enables study of PKS gene expression and the relationship to occurrence and biosynthesis of toxins. In future, the detection of toxin-related PKS transcripts in environmental samples, *e.g.,* by real-time reverse transcriptase polymerase chain reaction (Real-Time RT-PCR), may allow discrimination of toxin-producing from non-toxigenic algal strains.

The present study not only highlights the unique characteristics of dinoflagellate sequences, but also emphasises the potential for detecting a host of important functional genes from marine phytoplankton. We have demonstrated that random sequencing of cDNA libraries is an efficient tool to do so. In view of the enormous global ecological importance of dinoflagellates, diatoms and haptophytes in marine ecosystems, further molecular studies on these eukaryotic protists are definitely warranted. We have no doubt that the most interesting discoveries on the functional significance of these genes still lie ahead.

References

F. Crépineau, T. Roscoe, R. Kaas, B. Kloareg and C. Boyen, Plant Mol. Biol. 43, 503–513 (2000).

R.W. Eppley, Holmes and J.D.H. Strickland, Exp. Mar. Biol. Ecol. 1, 191–208 (1967).

R.R. Guillard and J.H. Ryther, Can. J. Microbiol. 8, 229–239 (1962).

M.D. Keller, R.C. Selvin, W. Claus and R.R.L. Guillard, J. Phycol. 23, 633–638 (1987).

M.S. Ko, Nuc. Acids Res. 19, 5705–5711 (1990).

K.L. Lidie, J.C. Ryan, M. Barbier, and F.M. Van Dolah. 2nd Symposium on Harmful Algae in the U.S., Woods Hole, MA Dec 8–15 (2003).

R. W. Litaker, P.A. Tester, A. Colorni, M.G. Levy and E.J. Noga, J. Phycol. 35, 1379–1389 (1999).

L. K. Medlin, W. H. C. F. Kooistra, D. Potter, G. Saanders and R. A. Wandersen, in: The origin of the algae and their plastids, D. Bhattacharya. Plant Systm. Evol. (Suppl.) 11,187–219 (1997).

D.W. Meinke, J.M. Cherry, C.D. Dean, S. Rounsley and M. Koornneef, Science 282, 662–682 (1998).

S. Scala, N. Carels, A. Falciatore, M.L. Chiusano and C. Bowler, Plant Physiol. 129, 993–1002 (2002).

F. Sterky, S. Regan, J. Karlson, M. Hertzberg, A. Rohde, A. Holmberg, B. Amini, R. Bhalerao, M. Larson, R. Villarroel, M. van Monagu, G. Sandberg, O. Olsson, T.T. Teeri, W. Boerjan, P. Gustafsson, M. Uhlén, B. Sundberg and J. Lundberg, Proc. Natl. Acad. Sci. USA 95, 13330–13335 (1998).

F.J.R. Taylor, Biosystems 13: 65–108 (1980).

K. Theodorides, A. DeRiva, J. Gómez-Zurita, P.G. Foster and A.P. Vogler, Insect Mol. Biol. 11, 467–475 (2002).

J.L.C. Wright and A.D. Cembella, in: Physiological Ecology of Harmful Algal Blooms, D. M. Anderson, G.M. Hallegraeff and A.D. Cembella, eds. (Springer-Verlag, Heidelberg), pp. 427–451 (1998).

Population Diversity of the Ostreopsidaceae in the Mediterranean Sea: A Preliminary Study on the Genetics and Morphology

Antonella Penna[1], Magda Vila[2], Maria Grazia Giacobbe[3], Elena Bertozzini[1], Francesca Andreoni[4], Santiago Fraga[5], Esther Garcés[2], Mercedes Masó[2], and Mauro Magnani[1]

[1]Centro Biologia Ambientale, University of Urbino, 61100 Pesaro, Italy; [2]Institut de Ciències del Mar, CSIC, 08039 Barcelona, Spain; [3]Istituto per l'Ambiente Marino Costiero, CNR, 98122 Messina, Italy; [4]Istituto Biotecnologie Agro-Industriali, University of Urbino, 61029 Urbino, Italy; [5]Instituto Español de Oceanografía, IEO, 36200 Vigo, Spain

Abstract

The relationships among different populations of *Coolia* Meunier and *Ostreopsis* Schmidt were investigated through the study of genetics and morphology. All the *Coolia* and *Ostreopsis* populations obtained from the Mediterranean and elsewhere were analysed by transmitted and epifluorescence light microscopy and nucleotide sequence alignments of the 5.8 S rDNA and internal transcribed spacer (ITS) regions.

Introduction

Ostreopsis and *Coolia* are two epiphytic/benthic dinoflagellates recorded together with *Gambierdiscus* and *Prorocentrum* in ciguatera-endemic, tropical areas. This group of dinoflagellates may be involved in the CFP (Ciguatera Fish Poisoning) complex and cause contamination of fish and seafood (Fukuyo, 1981). *C. monotis* is ubiquitous in tropical and temperate regions (Steidinger and Tangen, 1996), whereas *Ostreopsis* species are only documented in the ciguatera-endemic regions. Recently, *Ostreopsis* species occurrences have been recorded in temperate areas, such as the Western Mediterranean (Tognetto *et al.,* 1995, Vila *et al.,* 2001) and New Zealand (Rhodes *et al.,* 2000), as *O. ovata, Ostreopsis* sp. and *O. siamensis,* respectively. While the *Coolia* genus is easily identifiable by the plate tabulation, *Ostreopsis* morphology-based identification remains difficult, since several species are only distinguishable by shape, size and thecal pores (Faust *et al.,* 1996), which are variable both in cultures and in field samples. For this reason, recent studies combined both morphological and molecular analyses. In this study, we analyzed the genetic diversity of different isolates of *Ostreopsis* and *Coolia* species in the W Mediterranean by using the 5.8S rDNA and ITS regions, and then compared the W Mediterranean isolates with *Ostreopsis* and *Coolia* isolates outside the Mediterranean. The intra-species genetic variability among isolates was analyzed to partially establish the distribution pattern of different *Ostreopsis* and *Coolia* clades. The phylogenetic analyses were also useful to assess the taxonomic validity of the 5.8S rDNA and ITS markers at species level and clarify the morphology-based classification of *Ostreopsis* species.

Materials and Methods

Sample Collection and Microscopy *Coolia* and *Ostreopsis* cells were collected and isolated from net seawater samples or selected macroalgae (Rhodophyceae and Phaeophyceae) at specific places along the NW Italian and Spanish Mediterranean coasts. Clonal cultures of *Coolia* and *Ostreopsis* species (Table 1) were established in F/20 medium under alternating periods of 14 h light and 10 h dark (white fluorescence; 100 $\mu mol \cdot m^{-2} \cdot s^{-1}$) at 17 ± 1°C.

Species were identified based on epifluorescence morphological observations of plate patterns by using the calcofluor white staining method (Fritz and Triemer, 1985). The main literature used in species identification was Fukuyo (1981); Besada *et al.* (1982); Faust (1999).

Table 1 List of *C. monotis* and *Ostreopsis* spp. isolates obtained in this study.

Species	Strain Number	Sampling Location and Year	Culture Source	EMBL Accession No.
C. monotis	CNR-CMA4	Mediterranean, Ionian Sea, Italy, 2000	M.G. Giacobbe	AJ279032
C. monotis	IEO-CM2V	East Atlantic, Spain, 1985	I. Bravo	AJ319578
C. monotis	SZN-CM43	Mediterranean, Tyrrhenian Sea, Italy, 1998	M. Montresor	AJ308524
Ostreopsis sp.	CNR-B4	Mediterranean, Tyrrhenian Sea, Italy, 2000	E. Gangemi	AJ301643
Ostreopsis sp.	CSIC-D5	Mediterranean, Catalan Sea, Spain, 2000	E. Garcés	AJ312944
Ostreopsis sp.	CSIC-D7	Mediterranean, Catalan Sea, Spain, 2000	E. Garcés	AJ491334
O. cf. *ovata*	CNR-A1	Mediterranean, Tyrrhenian Sea, Italy, 2000	M.G. Giacobbe	AJ311520
O. cf. *ovata*	CNR-D1	Mediterranean, Ligurian Sea, Italy, 2000	M.G. Giacobbe	AJ320179
O. cf. *ovata*	IEO-OS01BR	West Atlantic, Brazil, 2000	S. Fraga	AJ420006
O. cf. *ovata*	IEO-OS02BR	West Atlantic, Brazil, 2000	S. Fraga	AJ491311

Steidinger, K. A., J. H. Landsberg, C. R. Tomas, and G. A. Vargo (Eds.). 2004. Harmful Algae 2002. Florida Fish and Wildlife Conservation Commission, Florida Institute of Oceanography, and Intergovernmental Oceanographic Commission of UNESCO.

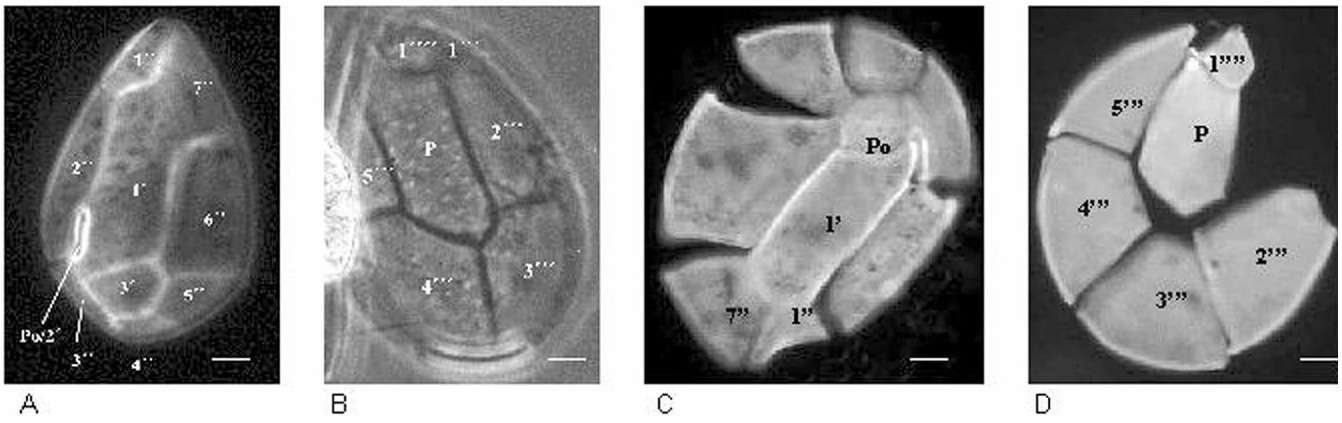

Figure 1 Thecal plate pattern of *Ostreopsis* sp. (**A**, **B**) and *O.* cf. *ovata* (**C**, **D**) from the W Mediterranean Sea. **A**, Apical view of *Ostreopsis* sp., field sample from Catalan Sea, Spain. **B**, Antapical view of *Ostreopsis* sp., field sample from Catalan Sea, Spain. Scale bars = 20 mm. **C**, **D**, Squashed epitheca and hypotheca of *O.* cf. *ovata* CNR-A1, clone from Tyrrhenian Sea, Italy. Scale bars = 10 μm.

PCR Amplification and DNA Sequencing Total DNA extraction, purification and amplification of the 5.8S rDNA and ITS regions were performed as described in Penna and Magnani (2000). Double-stranded PCR products were sequenced and aligned as described previously by Penna and Magnani (2001).

Phylogenetic Analyses Phylogenetic analyses were carried out using the distance method. Sequence alignment analyses were carried out by including other sequence data of *Ostreopsis* species and *C. monotis* from GenBank. The aligned data were converted to a distance matrix using the Kimura 2-parameter method of the neighbor joining, NJ function in the MEGA ver. 2 software (Kimura, 1980). The phylogenetic trees were constructed from the distance matrix using the NJ function of MEGA (Kumar *et al.,* 2001). A bootstrap analysis (1000 replications) was carried out to show the confidence in the branching order.

Results

Morphological Analyses In the W Mediterranean Sea, all *Ostreopsis* species analysed shared the same general plate pattern (Po, 3', 7'', 5''', 2'''', 1p). However, two *Ostreopsis* species have been distinguished by morphometric characters, as *Ostreopsis* sp. and *O.* cf. *ovata.* The dorso-ventral diameter (DV) of *Ostreopsis* sp. and *O.* cf. *ovata* were 63–90 and 27–65 μm, respectively. The antero-posterior diameter (AP) in *Ostreopsis* sp. was smaller than in *O.* cf. *ovata,* looking flat and ovoid, respectively. Few other differences were observed in the thecal tabulation or thecal structures (Fig. 1): the position of Po seemed to be a variable character for *Ostreopsis* sp. In general, it contacted 3' plate, but in a few cases there was no Po–3'contact (Fig. 1A). The *C. monotis* morphology of all isolates from the W Mediterranean was in accordance with the descriptions provided in literature and no morphological difference features were evident among these isolates (data not shown).

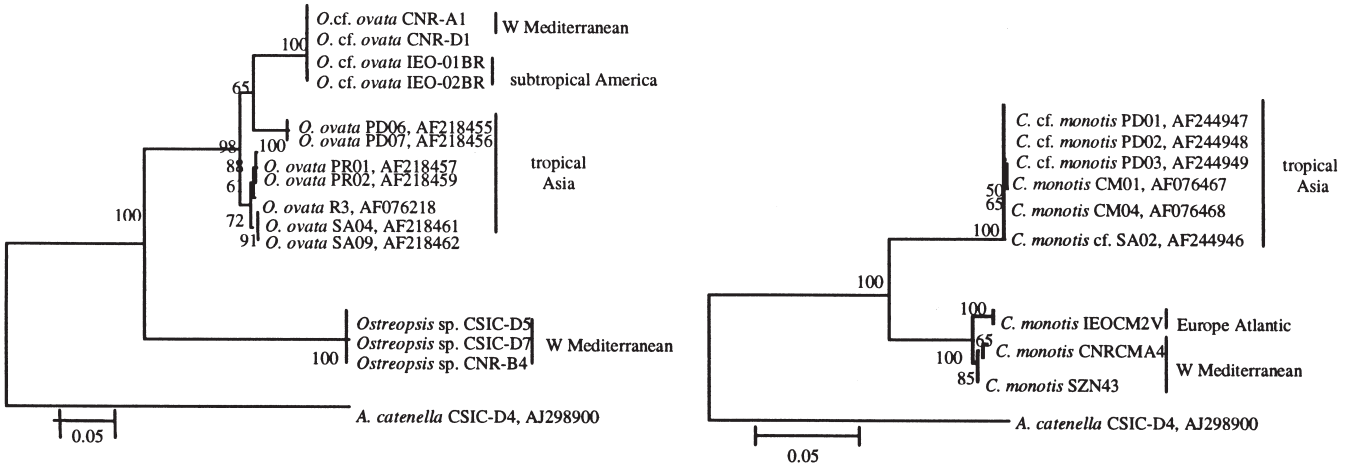

Figure 2 Phylogenetic trees inferred from the 5.8S rDNA and ITS regions in *Ostreopsis* species and *C. monotis* using the neighbor joining method. A distance of 0.05 is indicated by the scale. The numbers at nodes indicated the bootstrap values (≥ 50%). *Alexandrium catenella* CSIC-D4 was used as outgroup. Strain sequences obtained from GenBank contained accession numbers.

Molecular Analyses and Biogeographic Pattern Phylogenetic analyses inferred from the multiple sequence alignment of the 5.8S rDNA and ITS regions of the *Ostreopsis* and *C. monotis* isolates in the W Mediterranean are shown in Fig. 2. The *Ostreopsis* isolates clustered into two main groups in the W Mediterranean Sea: one group of *Ostreopsis* sp., with isolates from the Catalan and Sicilian coasts, and another group with *O.* cf. *ovata* isolates from the Ligurian and Tyrrhenian Seas; this was strongly supported by the bootstrap values (100%). All *C. monotis* isolates from the Mediterranean and Europe Atlantic grouped together with a marked divergence from the *C. monotis* populations from Asia. This was in accordance with the high bootstrap value (100 %).

Discussion

The identification of thecate dinoflagellates is based on the cell shape, surface ornamentation, position of the cingulum and plate pattern. However, for some species (*e.g., Ostreopsis* genus), the taxonomic classification based on the morphological characters is not an easy task. Here, the combined molecular and morphological characterisation was a good method to distinguish two morphospecies in the W Mediterranean Sea. *O.* cf. *ovata* fit well the description by Besada *et al.* (1982), despite the variability in cell size. The other species studied was *Ostreopsis* sp., the same species described in Vila *et al.* (2001). This species did not match any description well, although it was not far from the description of *O. siamensis* by Fukuyo (1981). All isolates of *Ostreopsis* sp. and *O.* cf. *ovata* from the W Mediterranean did not show any nucleotide difference within each group, with low values of the nucleotide diversity index (data not shown); the *Ostreopsis* sp. group, as well as *O.* cf. *ovata* group, were two homogenous clades. Furthermore, the *O.* cf. *ovata* clade from the W Mediterranean showed a high genetic similarity with the subtropical America *O.* cf. *ovata* isolates, clustering together. All populations of *O.* cf. *ovata* from W Mediterranean and subtropical America were clearly divergent from the *O. ovata* from Asia with a 98% of bootstrap value support, with the exception of two Asian isolates, *O. ovata* PD06 and *O. ovata* PD07; these resulted to be included in the W Mediterranean *O.* cf. *ovata* clade. In this study, the 5.8S rDNA and ITS region markers were useful for fine-scale population analyses of *Ostreopsis* spp. The genetic analyses were a useful tool to solve controversial on morphological and morphometrical-based identification. From these preliminary results the phylogenetic analyses showed that this genus is much more complex than it was assessed.

Within the Europe (W Mediterranean-Atlantic) group of *C. monotis* isolates, the results obtained from sequence comparison indicated that the isolates should be considered as a unique molecular type, according to the taxonomical classification in a single morphospecies, and separated from all Asian isolates. Also in this case, genetic markers were well exploited in the phylogenetic analyses of *C. monotis* isolates.

Acknowledgements

This work was supported by research funded by EU Strategy EVK3-CT-2001-00046 Project and MIPA V no. C58 under Ministero Politiche Agricole. We thank M. Montresor and I. Bravo for providing two culture strains.

References

E. G. Besada, L. A. Loeblich and A. R. Loeblich III, Bull. Mar. Sci. 32, 723–735 (1982).
M. A Faust, Phycologia 38, 92–99 (1999).
M. A Faust, S. L. Morton and J. P. Quod, J. Phycol. 32, 1053–1065 (1996).
L. Fritz and R. E. Triemer, J. Phycol. 21, 662–664 (1985).
Y. Fukuyo, Bull. Jpn. Soc. Sci. Fish. 47, 967–978 (1981).
M. Kimura, J. Mol. Evol. 16, 111–120 (1980).
S. Kumar, K. Tamura, I. B. Jacobsen and M. Nei, MEGA 2: Molecular Evolutionary Genetic Analysis Software, Arizona State University, Tempe, Arizona,USA (2001).
A. Penna and M. Magnani, in: International Conference on Harmful Algal Blooms, G. M. Hallegraeff, S. I. Blackburn, C. J. Bolch and J. Lewis, eds. (UNESCO, Paris), pp. 218–221 (2001).
A. Penna and M. Magnani, J. Phycol. 36, 1183–1186 (2000).
L. Rhodes, J. Adamson, T. Suzuki, L. Briggs and I. Garthwaite, N. Z. J. Mar. Freshwater Res. 34, 371–383 (2000).
K. A. Steidinger and K. Tangen, in: Identifying Marine Diatoms and Dinoflagellates, C. R. Tomas, ed. (Academic Press, New York), pp. 513–516 (1997).
L. Tognetto, S. Bellato, I. Moro, and C. Andreoli, Bot. Mar. 38: 291–295 (1995).
M. Vila, E. Garcés and M. Masó, Aquat. Microbiol. Ecol. 26, 51–60 (2001).

Species of *Pseudo-nitzschia* in the Drake Passage (54°–61°S to 46°–64°W)

Martha Ferrario[1], Sergio Licea[2], C. F. Balestrini[3] and Gustavo Ferreyra[3]
[1]*Facultad de Ciencias Naturales y Museo, Departamento Científico de Ficología, Paseo del Bosque s/n, 1900 La Plata, Argentina;* [2]*Instituto de Ciencias del Mar y Limnología, Apartado 70-305, México 04510, D.F.;* [3]*Instituto Antártico Argentino, Buenos Aires, Argentina*

Abstract

Previous studies of phytoplankton in the Drake Passage show that *Pseudo-nitzschia* species are an almost permanent component in Antarctic waters. This study shows that this genus is widely distributed and some of its species are present in high concentrations. Sampling for this study was surveyed aboard the icebreaker A.R.A. "Almirante Irizar" in the framework of the ARGAU project. Water and net samples were obtained during two cruises from January to May 2000–2001, respectively. Results revealed the presence of the species *P. turgidula* (Cleve) Hasle, *P. turgiduloides* (Hasle) Hasle, *P. lineola* (Cleve) Hasle, *P. heimii* Manguin and *P. dolorosa* sp. ined. Species were identified with both light (LM) and electron microscopes (TEM and SEM). Morphometric data and relative abundance are given.

Introduction

Hydrographic conditions in the Drake Passage are highly influenced by the circulation of the Antarctic marine water masses, as well as by the seasonal variation, which is more pronounced than interannual variability, giving to this region unique conditions that support a significant biological productivity (El Sayed and Mandelli, 1965; El Sayed *et al.,* 1977; Priddle, 1985). A relatively sharp temperature and salinity decrease, and chlorophyll *a* increase occurs at the Polar Front, located near 59° (Balestrini *et al.,* 2000). Early in the 1920s and 1930s the phytoplankton studies have been an important subject of investigation in this region (Hart 1934, Hendey, 1937), however, it is only recently that interest in harmful algae is increasing. The genus *Pseudo-nitzschia* has the most numerous species that produce domoic acid (DA), a toxin that causes Amnesic Shellfish Poisoning (Hasle *et al.,* 1996). Records of *Pseudo-nitzschia* in this geographic area are limited, restricted, or in a few cases included in the diatom lists (Kopczynska and Ligowski 1982, 1985; Medlin and Priddle, 1990). Because of the potential toxicity of the some of these species, this study was initiated with the purpose of tracing the distribution of this genus. The objective of this research is to know the taxonomy and occurrence of this group in the Drake Passage, and this is the first such study.

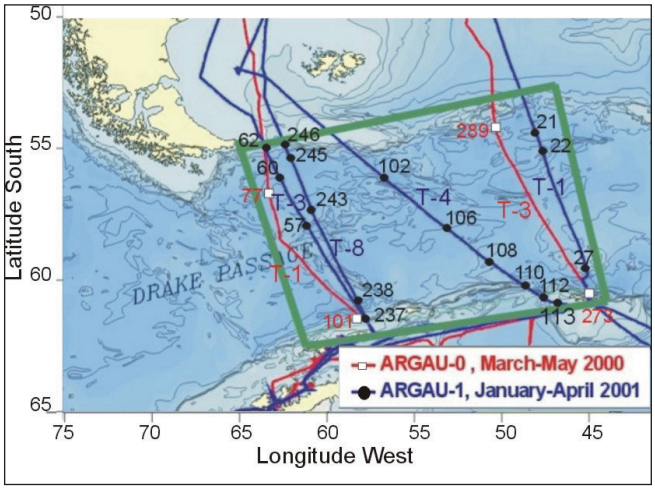

Figure 1 Sampling sites in the Drake Passage.

Materials and Methods

Samples for this study were obtained as part of the ARGAU project (Argentina for the study of the Austral Atlantic Ocean) in four selected transects of 10 stations each. Two cruises from January to May 2000–2001, respectively, were undertaken on board ARA "Almirante Irizar." The location of the fixed stations is given in Fig. 1.

Water samples for qualitative (30 µm net mesh) and quantitative analyses were taken by pumping water from an external intake located at nine depths using a continuous sampling system (Poisson *et al.,* 1993) and preserved with Lugol's solution. The preserved qualitative material was treated and mounted for light and electron microscopes according to Hasle and Fryxell (1970). The quantitative material was analyzed in an inverted microscope (Iroscope SI-PH). Samples were examined and photographed using the light microscope LM (Wild M20) and the scanning electron microscope (SEM: JEOL JSMT 100 at the Museo de La Plata). The transmission electron microscope (TEM: JEOL 1200 EX) was used. Material has been deposited in the collection of the Argentine Diatoms at the Department of Phycology, Faculty of Natural Sciences and Museum, The National University of La Plata. The terminology adopted here follows the proposals made by Hasle *et al.* (1996).

Results and Discussion

Quantitative analyses of phytoplankton of two cruises showed that *Pseudo-nitzschia* community was represented by *P. heimii. P. lineola, P. turgidula. P. turgiduloides* and *P. dolorosa* sp. ined., a new species proposed by Lundholm and Moestrup (pers. comm., Plate 1). In addition, some naked flagellates, cryptomonads, coccolitophorids and the diatoms—*Thalassiosira gracilis* (Karsten) Hustedt, var. *gracilis, Fragilariopsis kerguelensis* (O'Meara) Hustedt, *F. curta* (Van Heurck) Hustedt, *F.* aff. *separanda* Hustedt, *F.* Cylindrus (Grunow) Krieger, *Dactyliosolen antarcticus* Castracane, *D. tenuijunctus* (Manguin) Hasle, *Chaetoceros bulbosum* (Ehrenberg) Heiden, *C. atlanticus* Cleve and *C. socialis* Lauder—were present as well. Species distribution of *Pseudo-nitzschia* were similar to those reported by Kopczynska and Ligowski (1982, 1985) in February–March

Steidinger, K. A., J. H. Landsberg, C. R. Tomas, and G. A. Vargo (Eds.). 2004. Harmful Algae 2002. Florida Fish and Wildlife Conservation Commission, Florida Institute of Oceanography, and Intergovernmental Oceanographic Commission of UNESCO.

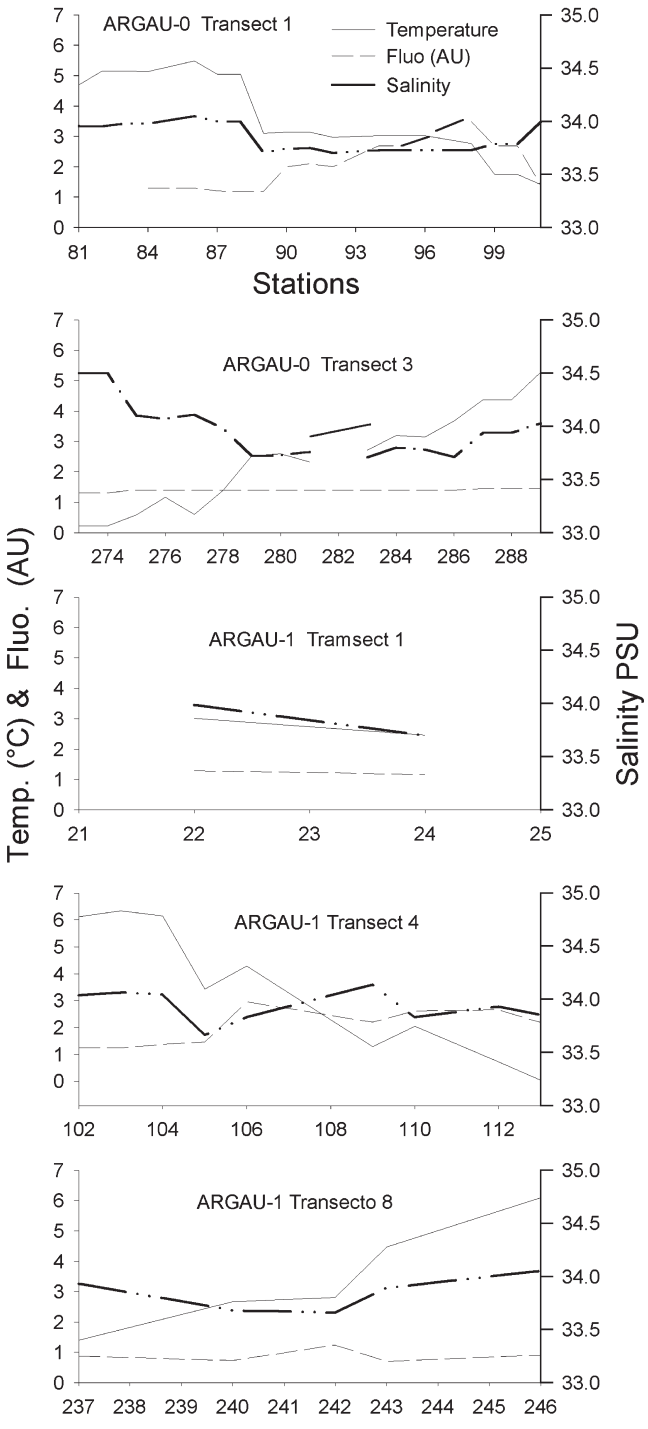

Figure 2 Spatial series of temperature, fluorescence and salinity of the ARGAU transects.

of 1981; however, the predominance of tiny flagellates and coccoid forms (<10 μm) in our net samples were not mentioned by those authors. When comparing our results of abundance and distribution of *Pseudo-nitzschia* with other authors, we observe that the species of *Nitzschia* of the group *Pseudo-nitzschia* and *Fragilariopsis* were usually included collectively within their groups, due to difficulties in identification when using only water mounts.

During the austral summer cruise (ARGAU-1), *P. turgidula* and *P. turgiduloides* were the most common species. In this period, maximum cell density was found in early summer with slightly higher values in late summer. *P. turgidula* has been reported as DA producer in coastal waters of New Zealand (Rhodes *et al.,* 1996). *P. heimii* was also well represented in this period as previously reported by Priddle (1985) in February–March of 1982 as *Nitzschia heimii.* This species registered the maximum abundance with 116.667 cells L^{-1} and a dominance of phytoflagellates at the end of February 2001 (587.302 cells L^{-1}) with a local temperature and salinity of 1.3°C and 34.13 PSU respectively, near the Polar Front. In contrast, *P. turgiduloides* showed the minimum abundance (1042 cells L^{-1}), associated with a decrease of phytoflagellates (123,333 cells L^{-1}), lower temperature (–0.75°C) and salinity (33.9 PSU), close to the Polar Front as well (Fig. 2). The quantitative analyses revealed that *P. heimii* and *P. turgiduloides* bloomed along all transects during the ARGAU-1 expedition (Table 1). In contrast, *P. dolorosa* is reported for the first time in sub-Antartic waters with very low abundance of cells at surface temperature of 6.4°C and 34.04 PSU. During the cruise ARGAU-O, *P. turgiduloides* and *P. turgidula* in transects 1 and 3 were the most abundant species; in contrast, *P. heimii* and *P. lineola* had less abundance and narrower distribution in the study area. Morphometric data revealed that the important characters to distinguish the species in this region are: the number of row of poroids, their size and shape, as well as the outline of the valve. These characters fit well for *P. lineola* and *P. turgiduloides,* in spite of its valve outline overlaps (Table 2).

Acknowledgements

This work was supported in part by grants from Argentina (CONICET, PIP 0947 and Mexico (Conacyt, J200.1326). We thank N. Lundholm and Ø. Moestrup for the confirmation of. *P. dolorosa* sp. ined.; N. Malacalza, R. Luna and M.E. Zamudio for their technical assistance.

Table 1 Maximum and minimum values of abundance (cells $10^3 \cdot L^{-1}$) of *Pseudo-nitzschia*.

	ARGAU-0				ARGAU-1			
Species	Max.	Sta.	Min.	Sta.	Max.	Sta.	Min.	Sta.
P. heimii	3.571	285	1.190	287	116.667	106	20.883	245
P. lineola	4.167	282	1.617	277	20.883	245	11.111	22
P. turgidula	10.753	98	1.190	286	83.333	106	2.778	110
P. turgiduloides	55.000	90	3.571	285	43.056	245	1.042	243
P. dolorosa sp. ined.					0.417			

Table 2 Morphometric data of *Pseudo-nitzschia* species in the Drake Passage.

Species	Length (µm) Min	Length (µm) Max	Width (µm) Min	Width (µm) Max	Striae in 10 µm Min	Striae in 10 µm Max	Fibulae in 10 µm Min	Fibulae in 10 µm Max	Poroids in 1 µm Min	Poroids in 1 µm Max	Rows of Poroids	Type of Poroids	Central Interspace
P. heimii	98	109	4.5	5.5	19	20	13	18	5	8	1–2	irregular	present
P. lineola	105	125	2.3	2.7	20	22	12	13	3	5	1	roundish	present
P. turgidula		50	2.7	3.0	20	24	13	14		8	2	irregular	present
P. turgiduloides	86	92	1.7	2.5	17	24	10	16	7	8	1–2	roundish	present
P-dolorosa sp. ined.	29	30	2.5	2.6	35	36	21		7	8	2	irregular	present

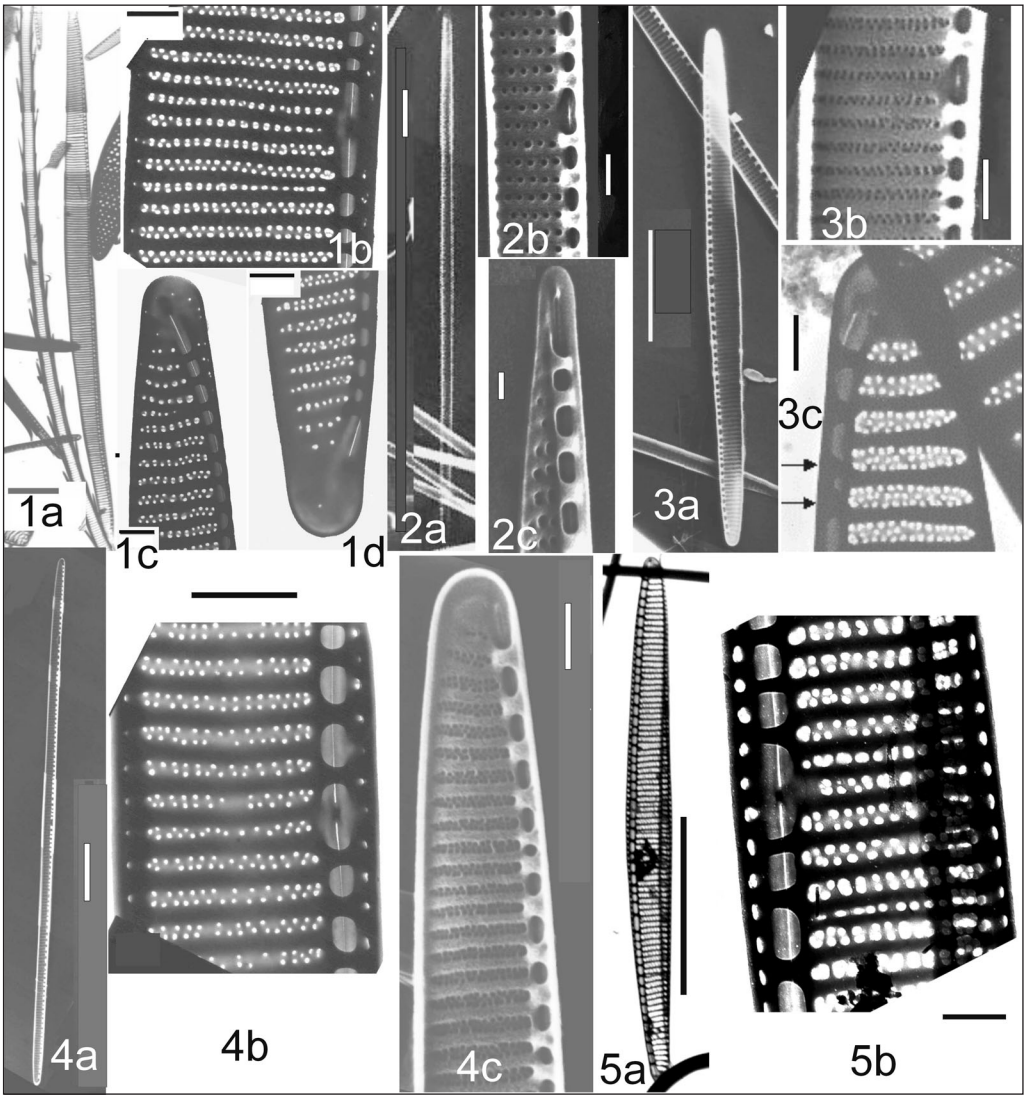

Plate 1: 1a *Pseudo-nitzschia heimii,* TEM, whole valve. **1b** Ibid., central part. **1c–d** Ibid., valve ends; note the valve heteropolarity. **2a** *P. lineola,* SEM, general internal view. **2b** Ibid., central part with central nodule and central inter-space. **2c** Ibid, valve end. **3a** *P. turgidula,* SEM, general internal view. **3b** Ibid., central part, internal; note fibulae with central inter-space and inter-striae. **3c** Ibid., TEM, valve end; **4a** *P. turgiduloides,* SEM, general internal view of whole valve. **4b** Ibid., TEM, central area. **4c** Ibid., SEM, internal view of the valve end. **5a** *P. dolorosa* sp. ined., TEM, whole valve; **5b** Ibid., central area. Scale bars = 10 mµ in figs. 1a, 2a, 3a, 4a, 5a. Scale bars = 1µ in others.

References

C. Ballestrini, A. Poison, G. Ferreyra, M. Ferrario, B. Schuer, I. Schloss, D. Molina, H. Sala, A. Bianchi, D. Ruiz-Pino, A. Piola and M. Sacaraceno, Int. Ant. Arg. 529, 1–30 (2000).

S. Sayed and E.F. Mandelli, Ant. Res. Ser. 5, pp. 87–106 (1965).

S. El-Sayed, Vol. 1, Scott Polar Res. Inst. Cambridge, pp. 1–79 (1977).

T.J. Hart, Discovery Rep. 8, pp. 268 (1934).

G.R. Hasle and G.A. Fryxell, Trans. Am. Microsc. Soc. 89, 4, 469–474 (1970).

G.R. Hasle, C.B. Lange and E.E. Syvertsen, Helgoländer Wiss. Meeresunters 50(2), 131–175 (1996).

E.Kopczynska and R. Ligowski, Polar Res. 3, 3–4, 193–202 (1982).

E. Kopczynska and R. Ligowski, Polar Res. 6, 1–2, 65–77 (1985).

N.I. Hendey, Discovery Rep. 16, pp. 151–364 (1937).

L.K. Medlin and J. Priddle, Polar Marine Diatom, British Antarctic Survey, pp. 214 (1990).

A Poisson, N. Metzl, C. Brunet, B. Shauer, B. Bres, D. Ruiz-Pino and F. Launchi, J. J. Geophys. Res. 22, 759–778 (1993).

J. Priddle, Meeresforschung 30, 240–250 (1985).

L.R. Rhodes, D. White, M. Sybre and M. Atkinson, In: Harmful and Toxic Algal Blooms. T. Yasumoto, Y. Oshima and Y. Fukuyo, eds. (IOC, UNESCO), pp. 155–158 (1996).

Genetic Variability and Toxin Profile of *Alexandrium tamarense* (Lebour) Balech from Southern Brazil

Graziela R. Persich[1], David M. Kulis[2], Emily L. Lilly[2], Donald M. Anderson[2], and Virgínia M.T. Garcia[1]
[1]*Fundação Universidade de Rio Grande (FURG), C. P. 474, 96201-900, Rio Grande, RS, Brazil;*
[2]*Woods Hole Oceanographic Institution, Biology Department, Woods Hole, MA 02543, USA*

Abstract

The distribution of the toxic dinoflagellate *Alexandrium tamarense* (Lebour) Balech has apparently expanded to or within the Southern Hemisphere during the last two decades. Toxic blooms of *A. tamarense* have been recorded in Argentinean coastal waters since 1980; however, the first documented bloom in southern Brazil was in 1996. In this study, 13 strains of *A. tamarense* from southern Brazil were isolated and kept in culture. Phylogenetic analysis using RFLP (Restriction Fragment Length Polymorphism) and DNA sequence of the D1-D2 region of large subunit ribosomal DNA (rDNA) places the Brazilian strains firmly within the North American clade, but does not assign them to any existing subclade. The cultures were also analyzed for saxitoxin and its derivatives by high performance liquid chromatography (HPLC). The main saxitoxin groups found were the low toxicity N-sulfocarbamoyl group C1+2 (30–84%), followed by the high potency carbamate toxins, gonyautoxins 1+4 (6.6–55%), gonyautoxins 2+3 (0.3–29%), neosaxitoxin (1.4–24%) and saxitoxin (0–4.4%). Toxin levels were variable (7,000 to 66,000 fg STX cell^{-1}), with the higher range falling among the most toxic values recorded for cultures of *A. tamarense,* indicating the significant risk for shellfish contamination and human intoxication during blooms of this species along the southern Brazilian coast. Possible dispersal hypotheses such as ballast water transport and natural mechanisms are also discussed.

Introduction

In South America, the range of *A. tamarense* appears recently to have spread around the southern tip and northward along the east coast. The earliest South American PSP outbreak was recorded in 1886 in Chile, associated with *A. catenella* (Sengers, 1908); the next outbreak was reported in 1972 (Guzmán *et al.,* 1975). In the South Atlantic, the first toxic outbreak of *A. tamarense* occurred in Argentina in 1980 (Carreto *et al.,* 1985); since then, this species has been periodically detected along that coast. In Uruguay, the first PSP outbreak also was recorded in 1980, but conclusive identification of *A. tamarense* as the causative species was not possible until the second toxic outbreak in 1991 (Brazeiro *et al.,* 1997). *A. tamarense* was first documented in southern Brazil in 1996, concomitant with a bloom in Uruguay (Odebrecht *et al.,* 1997). We hypothesized that the southern Brazilian *A. tamarense* populations were introduced by natural currents from Uruguay. This study represents the first attempt to isolate, determine the toxin composition profile, and uncover the origin of the *A. tamarense* population from southern Brazil, using both genetic analysis and historic accounts.

Materials and Methods

Origin of the Strains Sediment samples were collected from March to November, 1997 in Praia do Cassino (32°04′ to 32°30′S; 51°49′ to 52°10′W). Sediment cyst concentrations were estimated by counts in Sedgwick-Rafter chambers, following the staining method in Yamaguchi *et al.* (1995). Twelve clonal strains were developed by cyst isolation, germination and re-isolation of individual motile cells. Strain ATBRC6 was established from a vegetative cell isolated from the water column in August 1997. Cultures were kept in f/2 medium (-Si) at 20°C under a 14:10 h light:dark cycle and ca. 350 μE m^{-2} s^{-1} and were harvested for all analyses in mid-exponential growth phase.

Toxin Analysis Toxin analyses were carried out in triplicate using a modification of the Oshima (1995) post-column derivatization HPLC method (Anderson *et al.,* 1994). Unknowns were identified and quantified based on standard reference material provided by Y. Oshima, and the toxicity values, in saxitoxin equivalents, were converted from the molar concentrations using the factors found in Oshima (1995).

Genetic Analysis RFLP assays of LSU rDNA were performed using D1R and D2C primers and the enzymes *Nsp* 1, *Mse* 1, and *Apa* L1 according to Scholin and Anderson (1996). RFLP patterns from our strains were compared to published data (Scholin and Anderson 1996) and unpublished data generated by one of the authors (Lilly) for strains from Chile, Argentina and Uruguay. The entire D1-D2 region was sequenced for four strains, ATBR2c, 2d, 2e and 2f, and aligned with existing *Alexandrium* sequences from Scholin *et al.* (1994) and the sequence of a Chilean isolate (Lilly, unpublished data). The most appropriate substitution model was determined using ModelTest (Posada and Crandall, 1998). Using Paup version 4.0b8 (Swofford, 2002), one thousand replicates of maximum parsimony analysis were run to generate starting trees for maximum likelihood analysis. One hundred replicates of fast-step bootstrap were run using maximum likelihood.

Results

Cyst Distribution Cyst concentrations varied between undetectable values and 179 cysts cm^{-3} at the northern station (Fig. 1). These concentrations are substantially lower

Steidinger, K. A., J. H. Landsberg, C. R. Tomas, and G. A. Vargo (Eds.). 2004. Harmful Algae 2002. Florida Fish and Wildlife Conservation Commission, Florida Institute of Oceanography, and Intergovernmental Oceanographic Commission of UNESCO.

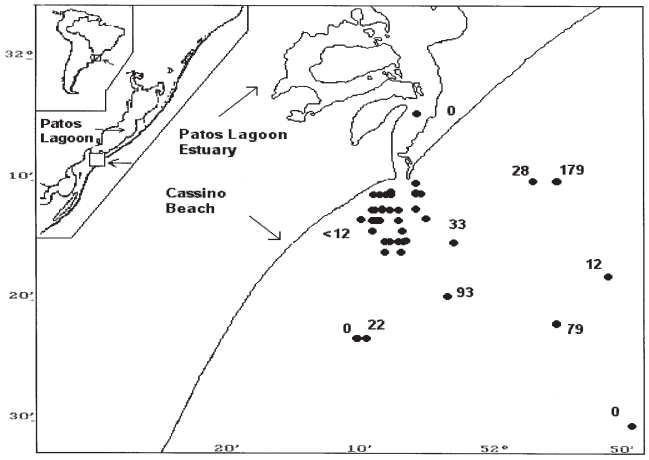

Figure 1 Sampling area with *A. tamarense* cyst concentrations (cysts cm^{-3}).

than the concentrations of cysts found in Argentina, which are up to 9,000 cysts cm^{-3} (Orozco and Carreto, 1987).

Toxin Analysis Total toxin concentration ranged from 42 to 199 fmol $cell^{-1}$ and toxicity from 7,000 to 65,900 fg STX eq $cell^{-1}$ in most of the strains, up to 78.4% of the total toxin (Fig. 2). The only exception was strain ATBRC6, whose higher toxicity value was due to the predominance of the potent GTX4.

Genetic Analysis RFLP analyses were inconclusive due to possible contamination issues. They indicated that the Western North American and the Eastern North American ribotypes might both be represented. Strains from Chile, Argentina and Uruguay display the Western North American ribotype (Lilly *et al.,* 2002). Sequence analyses were run on newly isolated material from four isolates that displayed the full range of patterns to clarify this issue. The sequences were identical to one another. The Brazilian sequences had several base changes in common with each of the Western, Eastern and Alternate North American ribotypes published by Scholin *et al.* (1994), but did not possess all of the base changes common to any of the groups. There was only one sequence difference with a Chilean strain. Phylogenetic analysis places the Brazilian strains firmly within the North American clade, but they do not fit within any existing subclade (Fig. 3).

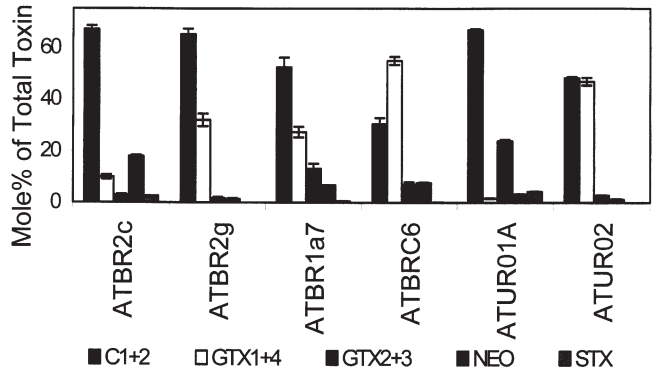

Figure 2 Toxin composition of representative Brazilian (ATBR) and Uruguayan (ATUR) strains.

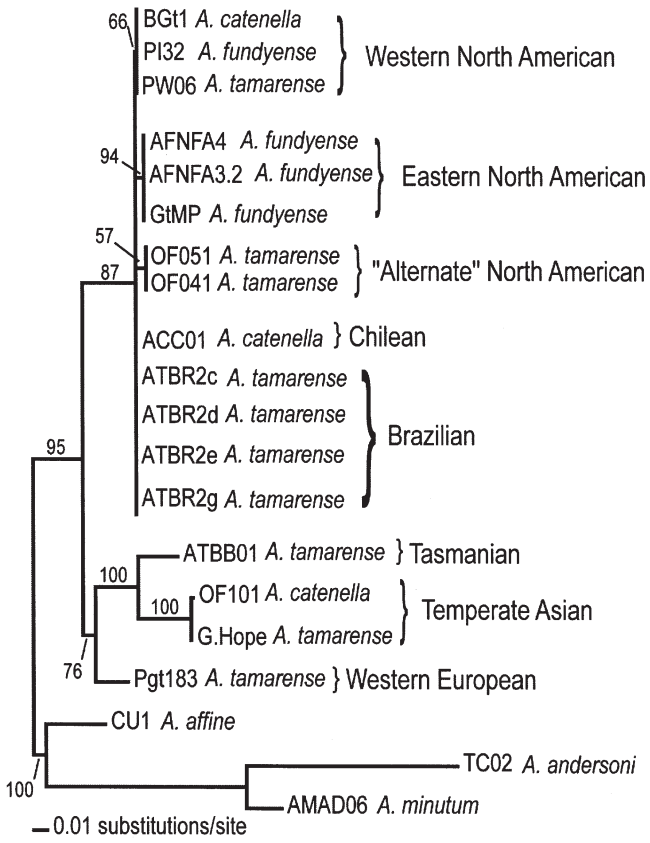

Figure 3 Maximum Likelihood tree showing the phylogenetic placement of the Brazilian strains within the *tamarensis* complex. Numbers represent 100 replicates of ML bootstrap.

Discussion

The occurrence of the North American pattern in *Alexandrium tamarense* from Brazil indicates a closer relationship with strains from the Northern Hemisphere than with strains from Australia or South Africa. Natural transport between North and South America in modern times is unlikely, since there are strong barriers, including temperature. One possible explanation could be that *Alexandrium* were transported in the ballast water of cargo vessels from the North American or Japanese coasts, where the North American ribotypes have also been detected (Scholin *et al.,* 1994). The other possibility is that the *Alexandrium* populations in South America were established much earlier during a period of cooler global ocean temperatures when natural transport across the hemispheres was possible, such as the last ice age. The DNA sequence data support this hypothesis. The South American LSU rDNA sequences are intermediate between the Asian, Western North American and Eastern North American populations of the North American ribotype, indicating that the populations have

been separated long enough for evolution to have occurred.

By either means, it is most likely that *A. tamarensis* complex cells first arrived in South America along the western coast and then spread to eastern South America via current systems. This is supported by the historical precedence of PSP in Chile, but not in other South American countries (Sengers, 1908, Guzmán *et al.,* 1975). PSP outbreaks subsequently occurred in Argentina, Uruguay and most recently, southern Brazil. Experimental and field observations also support this. First, there is the genetic pattern shared by the Chilean, Argentinean, Uruguayan and Brazilian strains, as shown with RFLP and sequence data (Lilly *et al.,* 2002). There is also a correlation of *Alexandrium* populations and presence of frontal systems in both Argentina and Uruguay (Carreto *et al.,* 1986 and Brazeiro *et al.,* 1997). Lastly, the high similarity between Brazilian and Uruguayan *Alexandrium* toxin profiles (present study and Mendéz *et al.,* 2001, respectively, Fig. 2) indicates a close relationship between these populations, as strains from each region have a high percentage of C1+2 toxins (30–80%), and lesser, but still an elevated mole percentage of the following toxins: GTX1+4 (2–55%), GTX2+3 (2–29%) and NEO (1–24%). Very low amounts of dcGTX3 and dcSTX and STX were seen in some of the isolates from each country as well.

Cyst concentrations in Brazilian sediments are lower than those in Argentina, but further study is needed to determine the reasons for this. Cultures derived from these cysts and vegetative cells can be highly toxic, with the higher range falling among the most toxic values recorded for *A. tamarense* cultures. In the future, we can expect additional toxic outbreaks from offshore cyst germination, or from new populations that are transported via Uruguayan coastal currents.

References

D. M. Anderson, D. M. Kulis, G. J. Doucette, J. C. Gallagher, and E. Balech, Mar. Biol. 120, 467–478 (1994).

A. Brazeiro, S. Mendéz and G. Ferrari, Atlântica 19, 19–29 (1997).

J. I. Carreto, R. M. Negri, H.R. Benavides and R. Akselman, in: Toxic Dinoflagellates, D. Anderson, A. White and D. Baden, eds. (Elsevier, Amsterdam), pp. 147–152 (1985).

J. I. Carreto, H. R. Benavides, R. M. Negri and P. D. Glorioso, J. Plankton Res. 8, 15–28 (1986).

L. Guzmán, I. Campodonico, M. Antunovic, Ans. Inst. Pat. Punta Arenas (Chile) 6, 209–223 (1975).

E. L. Lilly, K. Halanych and D. M. Anderson, this Proceedings.

S. Mendéz, D. M. Kulis and D. M. Anderson, in: Proceedings of the IX International Conference on HABs, G. M. Hallegraeff, C. J. Bolch, S. I. Blackburn and R. J. Lewis, eds, (UNESCO), 352–355 (2001).

F. E. Orozco and J. I. Carreto, in: Red Tides: Biology, Environmental Science and Toxicology, T. Okaichi, D. M. Anderson and T. Nemoto, eds. (Elsevier, New York), pp. 309–312 (1988).

Y. Oshima, in: Manual on Harmful Marine Microalgae, G. M. Hallegraeff, D. M. Anderson and A. D. Cembella, eds., UNESCO, pp. 81–94 (1995).

Posada, D., and Crandall, K. A. Modeltest: testing the model of DNA substitution. Bioinformatics 14: 817–818 (1998).

Swofford, D. PAUP: Phylogenetic analysis using parsimony. Sinauer Associates, Sunderland, MA. 4.0b10 (2002).

Formation of *Dinophysis dens* Pavillard and *D. diegensis* Kofoid from Laboratory Incubations of *Dinophysis acuta* Ehrenberg and *D. caudata* Saville-Kent

Beatriz Reguera[1], Sonsoles González-Gil[1], and Maximino Delgado[2]
[1]*Instituto Español de Oceanografía, Centro Oceanográfico de Vigo, Aptdo. 1552, 36280 Vigo, Spain;*
[2]*Centre d'Aqüicultura-IRTA, Generalitat de Catalunya, Sant Carles de la Ràpita, Spain*

Abstract

Vegetative cells of several species of *Dinophysis* spp. have been found to produce "small cells," different in size and shape, following a "reductionary division" under certain environmental conditions, as part of a polymorphic life cycle. Based on observations on fixed natural populations, *Dinophysis dens* and *D. diegensis* were hypothesized to be small forms of *Dinophysis acuta* and *Dinophysis caudata,* respectively. During autumn 2001, we were able to confirm these hypotheses after incubations, in cell culture chambers, of groups of individually picked cells from natural populations of *D. acuta* and *D. caudata*. Eight to 10 days after inoculation, different life cycle stages of the two species were observed *in vitro* and contrasted with wild specimens from *Dinophysis* blooms in Galician and Catalan waters.

Introduction

Dinophysis acuminata, D. acuta and *D. caudata* produce lipophilic toxins (Fernández *et al.,* 2001, submitted), leading to prolonged closures of shellfish beds in Galicia. Large intraspecific morphological variability has been observed in these three species (Reguera and González-Gil, 2001), leading to uncertainties in their taxonomic classification, based on the size and shape of the large hypothecal plates and sulcal lists. The problem is exacerbated when intraspecific variability is added to the difficulties met in routine monitoring analyses to separate two closely related species, such as the pair *D. acuminata* /*D. sacculus* (Zingone *et al.,* 1998) and *D. caudata* / *D. tripos* (Reguera and González-Gil, 2001). A great deal of intraspecific variability within the same region can be explained by complex polymorphic life cycles within *Dinophysis* spp. that include formation of small and intermediate cells, different in size and shape from the vegetative cells (Reguera and González-Gil, 2001). The formation of small (*D. skagii*-like) cells that behave as male gametes, following a "reductionary division" of a large cell, and of intermediate cells, formed after growth of the small cells, have been demonstrated by the latter authors after laboratory incubations of single cell isolates of *D. acuminata*. In this paper, we confirm with laboratory incubations that *D. dens* Pavillard and *D. diegensis* Kofoid that had been hypothesized (from observations on fixed field samples) to be conspecific with *D. acuta* Ehrenberg and *D. caudata* Saville Kent, respectively, are but life cycle stages of these species. Illustrations of small and intermediate forms of *D. caudata* and *D. acuta* are contrasted with those observed during their proliferation in Galicia or Catalonia.

Materials and Methods

D. caudata and *D. diegensis*-like specimens observed in a hose sample during monitoring in the Ebro Delta (Catalonia) in October 1997 (Delgado *et al.,* 2002) were filtered through a 10-µm mesh and stained with calcofluor (Fritz and Triemer, 1985). 70 selected images of *D. caudata*/*D. diegensis* were taken at 1000 X and the contours of the hypothecal plates redrawn on the computer. Bottle samples with *Dinophysis* spp. from the Galician rías (October 2001) were concentrated through a 20-µm mesh. Full-sized healthy (well-pigmented and mobile) vegetative cells of *D. acuta* and *D. caudata* were picked with microcapillary pipettes under an inverted microscope (25×, 100×), transferred 2–3 times through filtered (0.2 µm Millipore filters) seawater and placed in groups of 12–15 cells in 0.2 mL wells of culture plates with modified L1 culture medium, as in Reguera and González-Gil (2001). They were further incubated at 15°C (+ 1°C) and a 16:8 L/D regime, and examined daily with an inverted microscope (100×) (*D. acuta*) or with a stereomicroscope (40×) (*D. caudata*). Several times, the content of one well was collected and fixed with buffered formaldehyde for detailed microscopic observation and measurements of digitized images, obtained with a Sony Hi Resolution CCD-IRIS video system (Sony Corp., Japan) connected to the microscope, and to an image analysis programme (IPPLUS 4.0).

Results and Discussion

The sample from Delta del Ebro corresponded to late stages of a *D. caudata* + *D. diegensis* population (693 cell·L^{-1}) that lasted from August to October 1997. 76% of the specimens were vegetative cells of *D. caudata* and 24% were *D. diegensis*-like cells and intermediate forms between the latter and *D. caudata.* Thus, a large variability was observed in the size (L:35–79 µm; W:15–41 µm) of the large hypothecal plates, in the curvature of the dorsal margin and in the differentiation of the antapical process of these specimens (Fig. 1) that included forms illustrated by Jorgensen as *Dinophysis caudata* var. *subdiegensis, D. diegensis, D. caudata* a degenerate form, *D. caudata* var. *abbreviata* and *D. caudata* var. v*entricosa* (Figs. 31–32 and 35–37 in Jorgensen, 1923). *D. tripos,* a species with small and intermediate forms that can easily be mistaken for those of *D. caudata* (Reguera and González-Gil, 2001), was never observed in the area during the sampling period. Fig. 2 illustrates wild and laboratory incubated specimens of *D.*

Steidinger, K. A., J. H. Landsberg, C. R. Tomas, and G. A. Vargo (Eds.). 2004. Harmful Algae 2002. Florida Fish and Wildlife Conservation Commission, Florida Institute of Oceanography, and Intergovernmental Oceanographic Commission of UNESCO.

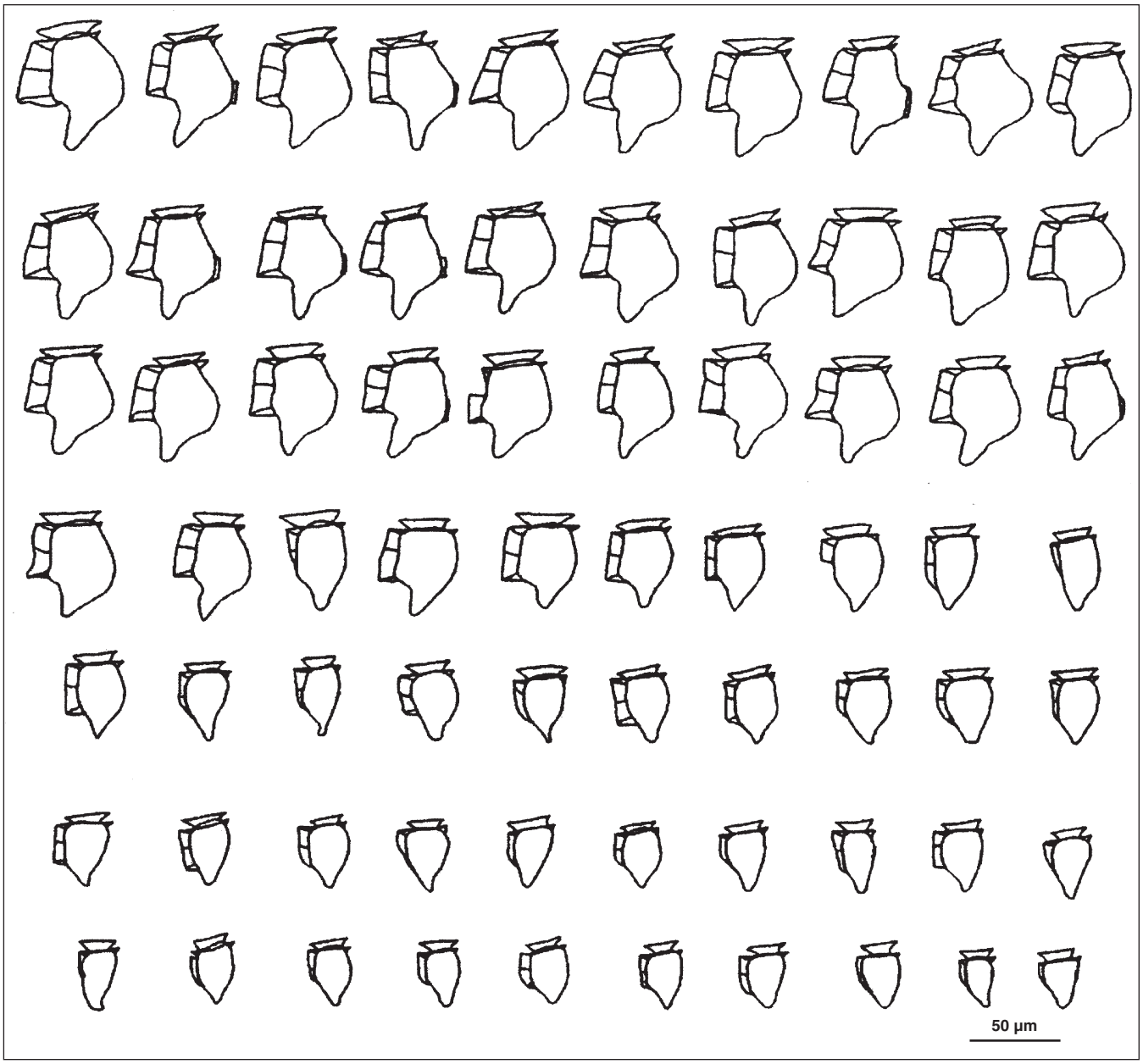

Figure 1 Micrograph contours of *D. caudata* (rows 1–3), *D. diegensis* (rows 6–7) and intermediate forms between *D. caudata* and *D. diegensis* (rows 4–5) found in a single sample from Delta del Ebro (Southern Catalonia, Spain, Mediterranean coast) that correspond to late stages of a *D. caudata* population.

caudata, D. acuta, and their respective small forms obtained from the rías of Vigo and Pontevedra (Galicia, Spain). Vegetative cells of *D. caudata* (L:79–87 µm; W:35–44 µm) and its small cells (L:50–68 µm) were larger and wider than those from Catalonia, but in both cases the vegetative cells were similar to those of *D. caudata* var. *abbreviata* sensu Jorgensen (1923). Vegetative cells of *D. acuta* from Galicia measured L:67 ± 3 µm (63–73 µm); W:47 ± 2 µm (46–54 µm), and those of *D. dens* L:43–47 µm; W:28–34 µm. Incubated *D. caudata* individual and paired cells were extremely buoyant and had to be observed from above with a stereomicroscope. Eight to 10 days after inoculation, small cells similar to *D. diegensis* and *D. dens* started to appear and eventually dominated the population in wells where *D. caudata* and *D. acuta* respectively had been inoculated. Cells going through a "reductionary division," couplets *D. caudata–D. diegensis,* and the large cell engulfing the small one were also observed. The observation of these forms after incubation of individually picked vegetative cells of *D. acuta* and *D. caudata* confirms, as it was previously hypothesized, that they are part of a polymorphic life cycle of these species of *Dinophysis.*

Acknowledgements

We thank P. Lourés for technical assistance, the crew of R.V. *J. M. Navaz* and the CCMM (Xunta de Galicia) for weekly information on phytoplankton. This research was funded with project MAR99-0224.

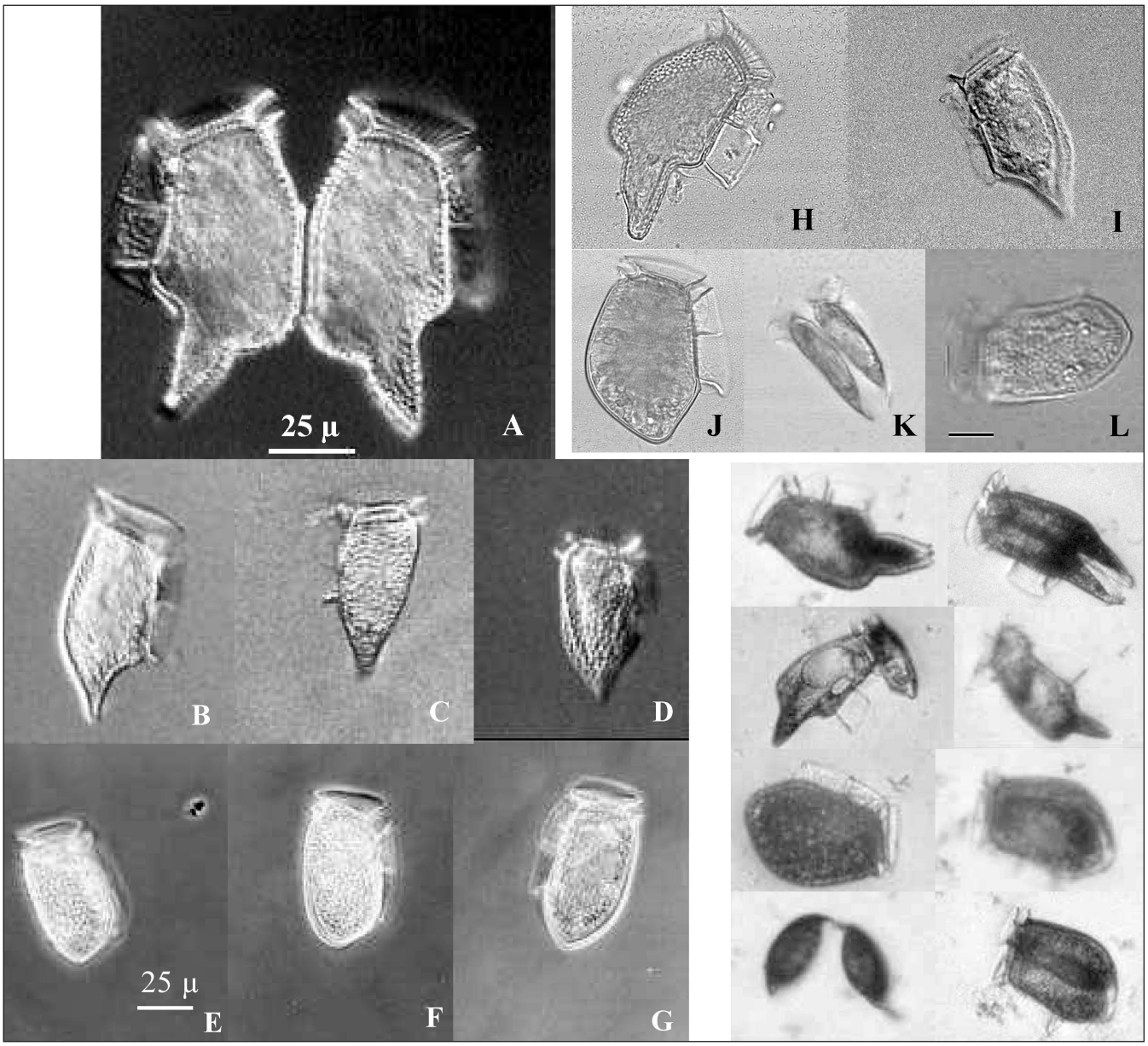

Figure 2 **A**–**D**: Light (DIC) micrographs of *Dinophysis caudata* and *Dinophysis diegensis*-like cells from Ría de Vigo: **A**, fully developed vegetative pair of *D. caudata;* **B**, intermediate form between *D. caudata* and *D. diegensis;* **C**–**D**, *D. diegensis*-like small cells. **E**–**F**, phase contrast micrographs of *D. dens;* **G**, intermediate form between *D. dens* and *D. acuta* (bar = 25 µm). **H**–**L**: digitized micrographs of incubated specimen: **H**, vegetative cell of *D. caudate;* **I**, *D. diegensis*-like cell formed after incubation of *D. caudata* specimen; **J**, vegetative cell of *D. acuta;* **K**, paired cells of *D. acuta* through a "reductionary" division leading to formation of small *D. dens*-like cells; **L**, *D. dens*-like cell formed after incubation of *D. acuta* cells (bar = 20 µm). Bottom right: Low-resolution micrographs (100×) of live specimen of *D. caudata* and *D. acuta* swimming in the incubation wells: first row: Dividing cells of *D. caudata;* second row: two steps of the fusion of a *D. caudata* with a *D. diegensis*-like cell formed after 8 days of incubation of vegetative cells; third row: heavily pigmented (planozygote?) and a normal vegetative cell of *D. acuta;* fourth row: Paired cells of *D. acuta* completing cytokinesis.

References

M. Delgado, M. Vila, E. Garcés and J. Camp, in: VI Reunión Ibérica sobre Fitoplancton Tóxico y Biotoxinas, Junta de Andalucía, Consejería de Agricultura y Pesca, ed., Congresos y Jornadas 55/00, pp. 219–222 (2002).

M. L. Fernández, B. Reguera, I. Ramilo and A. Martínez, in: Harmful Algal Blooms, G. Hallegraeff, S. Blackburn, R. Lewis and C. Bolch, eds., IOC of UNESCO, Paris, pp. 360–363 (2001).

M. L. Fernández, B. Reguera, S. González-Gil and A. Míguez, Toxicon (submitted).

L. Fritz and R. F. Triemer, J. Phycol. 21, 662–664 (1985).

E. Jorgensen, Rep. Dan. Oceanogr. Exped. 2 (J2), 1–48 (1923).

B. Reguera and S. González-Gil, J. Phycol. 37, 318–333 (2001).

A. Zingone, M. Montresor and D. Marino, Eur. J. Phycol. 33, 259–273 (1998).

Taxonomic Re-evaluation of a South Carolina "Red Tide" Dinoflagellate Indicates Placement in the Genus *Kryptoperidinium*

Jennifer L. Wolny[1], Jason W. Kempton[2], and Alan J. Lewitus[2,3]

[1]*Florida Fish and Wildlife Conservation Commission and Florida Institute of Oceanography, 100 8th Ave. SE, St. Petersburg, FL 33701, USA;* [2]*South Carolina Department of Natural Resources, 217 Ft. Johnson Rd., Charleston, SC 29422, USA;* [3]*Belle W. Baruch Institute for Marine Biology and Coastal Research, University of South Carolina, P.O. Box 1630, Georgetown, SC 29442, USA*

Abstract

"Red tides" occurring in South Carolina (SC) estuaries since 1998 have been associated with shellfish mortality events in the field and sublethal effects in laboratory bioassays. Initially, the dinoflagellate responsible for these blooms was identified as a new *Scrippsiella* species. Recent morphological and molecular studies have produced evidence that this dinoflagellate belongs in the genus *Kryptoperidinium.* Light and scanning electron microscopy show similarities in cell morphology and plate tabulation to published descriptions of *K. foliaceum.* Nuclear SSU and ITS rDNA sequence data are identical to a known strain of *Peridinium* (*Kryptoperidinium*) *foliaceum* (UTEX LB 1688). However, the UTEX LB 1688 strain has an endosymbiotic nucleus, whereas the SC bloom dinoflagellate does not, stressing the need to re-evaluate the taxonomic relevance of endosymbiotic features in this genus. In summary, the morphological and molecular data support the placement of this dinoflagellate in *Kryptoperidinium.*

Introduction

Since 1998, South Carolina (SC) estuaries from Murrells Inlet to Hilton Head (Fig. 1) have experienced recurrent "red tides" caused by a small, lightly armored dinoflagellate. These widespread blooms are characterized by patchy, rust to bright orange colored waters that appear in tidal creeks throughout the spring and summer. Blooms have been associated with shellfish mortality events, significantly reduced growth in juvenile hard clams, and physiological stress in oysters (Lewitus and Holland 2003; Lewitus *et al.,* 2003). Observations of these blooms have increased annually in frequency and areal extent since their initial discovery (Lewitus and Holland 2003). Based on the initial evaluation of thecal plates, Lewitus *et al.* (2001) reported this dinoflagellate as a new species, *Scrippsiella carolinium* sp. nov. At the time of that report, a formal description of the species was in preparation. Upon further evaluation, it was determined that the species was *Kryptoperidinium foliaceum* (Stein) Lindemann. Therefore, *S. carolinium* sp. nov. is a *nomen nudem;* an available but invalid name. Here we report morphological and molecular data indicating that the "SC bloom dinoflagellate" belongs in the genus *Kryptoperidinium* Lindemann.

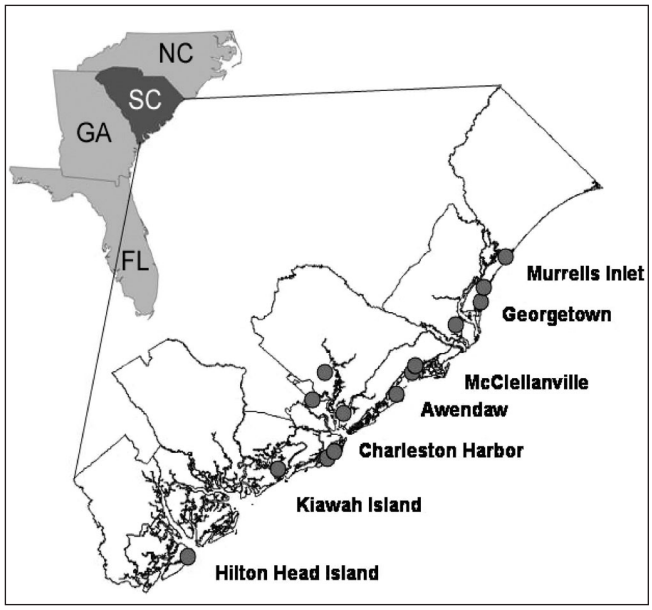

Figure 1 The 260 km of SC coastline experiencing red tides from spring 1998 through summer 2002.

Materials and Methods

Live and preserved samples from several coastal locations were chosen based on cell concentration (>100 cells/mL) and cell health (>50% of cells were vegetative swimming cells vs. temporary cysts). Fresh samples were collected as surface water grab samples in 1-L acid-washed bottles. Unpreserved samples were immediately screened using light microscopy for the presence of the SC bloom dinoflagellate. Aliquots of appropriate samples were stained with Calcofluor White for observation following the methods of Fritz and Triemer (1985) and then preserved with Lugol's iodine solution for future evaluations. Morphological comparisons were made between field material and four reference cultures of *K. foliaceum.* Comparative data to UTEX LB 1688 (*P. foliaceum*) are presented here.

Comparisons of nuclear SSU rDNA sequence data were made using eukaryotic-specific primers (Medlin *et al.,* 1988; Sogin 1990) coupled with species–specific primers designed for *K. foliaceum* (Kempton *et al.,* 2002). *K. foliaceum* primers were selected based on sequence data deposited in GenBank for UTEX LB 1688 (Inagaki *et al.,* 2000; Accession #AF231804). PCR reaction conditions and reagent concentrations followed methods described by Rublee *et al.* (1999). The internal transcribed spacer regions (ITS1 and ITS2) and 5.8S rRNA were sequenced for the SC bloom dinoflagellate and UTEX LB 1688 using a dinoflagellate-

Steidinger, K. A., J. H. Landsberg, C. R. Tomas, and G. A. Vargo (Eds.). 2004. Harmful Algae 2002. Florida Fish and Wildlife Conservation Commission, Florida Institute of Oceanography, and Intergovernmental Oceanographic Commission of UNESCO.

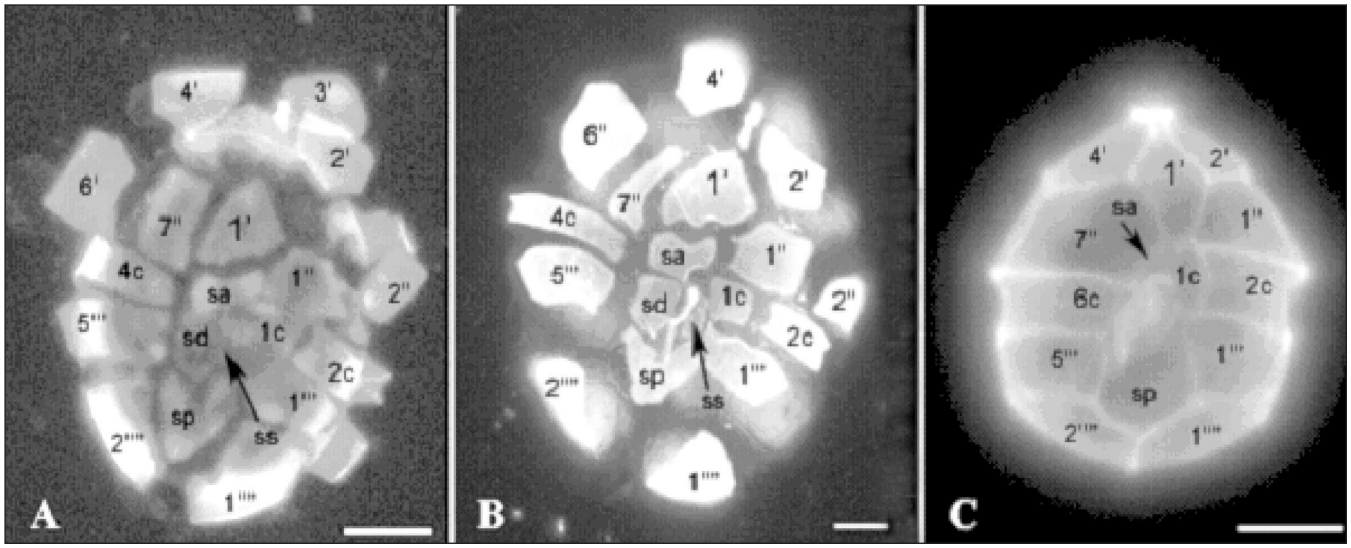

Figure 2 Calcofluor White images showing the shape and arrangement of the apical, cingular, and sulcal plates of **A** SC bloom dinoflagellate, **B** *P. foliaceum* strain UTEX LB 1688, and **C** *Scrippsiella precaria* strain JW010818-1C5. Scale bar = 10µ.

specific primer (Dino F, Oldach *et al.,* 2000) coupled with general primers for sequencing the ITS regions (Kempton *et al.,* 2002).

All microscopy and genetics methods are described in detail in Kempton *et al.* (2002).

Results and Discussion

Morphologically, the SC bloom dinoflagellate resembles the description for *K. foliaceum* (Basyionym: *Glenodinium foliaceum* Stein; Synonyms: *Peridinium foliaceum* (Stein) Biecheler, *Phyllodinium scutellaris* Conrad) by Biecheler (1952) and Sournia (1986). Biecheler (1952) and Sournia (1986) state that *K. foliaceum* has a rounded epitheca, a round to oblong hypotheca, is extremely dorso-ventrally compressed (concave ventral and convex dorsal surfaces), and has a large, conspicuous eyespot in the longitudinal furrow of the sulcus. Sournia (1986) reports a size range of 15–50 µm; the average SC bloom dinoflagellate cell diameter is 26.6 µm (range 10 µm–51 µm; 100 cells).

Evidence from light microscopic examination of field samples and cultures further supports the placement of this dinoflagellate into the monospecific genus *Kryptoperidinium.* We determined the following thecal plate pattern for the SC bloom dinoflagellate and UTEX LB 1688: Po, X, 4', 2a, 7", 4c, 4 or 5s, 5'", 2"" (Figs. 2A,B). This is similar to the pattern described for *K. foliaceum* by Biecheler (1952) and Sournia (1986), who both mention the possibility of 3 to 4 apical plates, 2 anterior intercalary plates, 6 to 7 precingular plates, 5 postcingular plates, and 2 antapical plates. Biecheler (1952) states that the sulcus consists of 2 plates and does not address the cingular plate series. Sournia (1986) only mentions that the sulcal and cingular plates need to be described.

In contrast, the plate pattern for the genus *Scrippsiella* Balech ex Loeblich III is Po, X, 4', 3a, 7", 6c, 4–5s, 5'", 2"" (Steidinger 1997), differing from *K. foliaceum* in the number of anterior intercalary (a) and cingular (c) plates and arrangement of the sulcal (s) plates (Fig. 2C). The SC bloom dinoflagellate has 2a plates, whereas *Scrippsiella* has 3a plates. The cingular series consists of 4 plates in the SC bloom dinoflagellate and 6 plates in *Scrippsiella.* Both genera have 4 or 5 sulcal plates; however, the posterior sulcal (sp) plate contacts the 1c plate in *Scrippsiella* species (Steidinger 1997). The sp plate in the SC bloom dinoflagellate is separated from the cingulum by the right (sd), left (ss), and median (sm) sulcal plates. Descriptions by Biecheler (1952) and Sournia (1986) mention that *K. foliaceum* has an incomplete cingulum. We have determined that this "incomplete cingulum" is the result of the large size of both the anterior sulcal (sa) and sd plates, which extend above and below the cingular margins (Figs. 2A,B). Other differences between these two genera include the shape and arrangement of the 1' plates. *Scrippsiella* species are described as having narrow, symmetrical to slightly asymmetrical, ortho-arranged 1' plates (Honsell and Cabrini 1991, Steidinger 1997). *Scrippsiella precaria* Montresor and Zingone has a diamond shaped 1' plate that is in contact with the cingulum (Fig. 2C). Like *K. foliaceum,* the SC bloom dinoflagellate has an ortho-arranged, wide, asymmetrical 1' plate that joins with the sa plate, not the cingulum (Figs. 2A,B).

The similarity between the SC bloom dinoflagellate and *K. foliaceum* was further examined by comparing nuclear SSU rDNA sequence data. Sequence data derived from the SC bloom dinoflagellate differed from the UTEX LB 1688 sequence data, as reported in Inagaki *et al.* (2000, Accession #AF231804), by 4 base pairs. However, sequence data from the SC bloom dinoflagellate were identical to sequence data deposited in GenBank for UTEX LB 1688 by Saldarriaga *et al.* (2001, Accession #AF274268). The ITS sequence data were also found to be identical for the SC bloom dinoflagellate and the UTEX LB 1688 strain, fur-

ther supporting the conclusions from the morphological comparisons that the SC bloom dinoflagellate belongs in the genus *Kryptoperidinium.*

Despite the similarity in SSU and ITS rDNA sequences and thecal plate tabulation, one morphological inconsistency between the SC bloom dinoflagellate and the UTEX LB 1688 strain of *P. foliaceum* is worth noting. Using a modified preserving method and DAPI nuclear staining protocol, it was determined that the SC bloom dinoflagellate lacks the endosymbiont nucleus that is present in UTEX LB 1688 (Kempton *et al.,* 2002). The taxonomic relevance of this feature for establishing *Kryptoperidinium* phylogeny is unclear.

In conclusion, morphological (*e.g.,* thecal plate pattern) and molecular (nuclear SSU and ITS rDNA sequences) data support the placement of the SC bloom dinoflagellate in the genus *Kryptoperidinium* and not in *Scrippsiella* (as reported in Lewitus *et al.,* 2001). Further research is needed on the *Kryptoperidinium* clade in order to determine whether this is a monospecific genus (*e.g.,* see Kempton *et al.,* 2003) and to explore taxonomic and evolutionary relationships between *K. foliaceum* strains with and without the endosymbiont nucleus.

Acknowledgements

We thank P. Scott, J. Tunnell, and K. Steidinger (FMRI/FIO), T. Tengs (University of Oslo), L. Schmidt (Baruch Institute), and R. Morris and P. Rizzo (Texas A&M University) for assistance with analyses. This study was funded by ECOHAB grant NA860P0493, NOAA grants NA90AA-D-SG672 and NA06OA0675, SC Sea Grant Consortium grant NA86RG0052, and a CDC grant to SC Department of Health and Environmental Control. ECOHAB Contribution 90, Contribution 1377 of the Belle W. Baruch Institute for Marine Biology and Coastal Research, and Contribution 532 of SCDNR Marine Resources Research Institute.

References

B. Biecheler, Bull. Biol. France Belgique. Suppl., 1–149 (1952).
L. Fritz and R. Triemer, J. Phycol. 21, 662–664 (1985).
G. Honsell and M. Cabrini, Bot. Mar. 34, 167–175 (1991).
Y. Inagaki, J. Dacks, W. Doolittle, K. Watanabe and T. Ohama, Intl. J. Syst. Evol. Microbiol. 50, 2075–2081 (2000).
J. Kempton, J. Wolny, T. Tengs, P. Rizzo, R. Morris, J. Tunnell, P. Scott, K. Steidinger, S. Hymel, and A. Lewitus, Harmful Algae 1, 383–392 (2002).
J. Kempton, P. Williams, S. Wilde, J. Wolny, and A. Lewitus, this Proceedings.
A. Lewitus, K. Hayes, S. Gransden, H. Glasgow, J. Burkholder, P. Glibert and S. Morton, Proceedings of the IXth International Conference on Harmful Algal Blooms, G. Hallegraeff, S. Blackburn, C. Bolch and R. Lewis, eds. (IOC UNESCO, Paris), pp. 129–132 (2001).
A. Lewitus and A. Holland, Proceedings of the EMAP Symposium 2001: Coastal Monitoring Through Partnership; Environmental Monitoring and Assessment 81, 361–371 (2003).
A. Lewitus, L. Schmidt, L. Mason, J. Kempton, S. Wilde, J. Wolny, B. Williams, K. Hayes, S. Hymel, C. Keppler, and A. Ringwood, Popul. Environ. 24, 387–413 (2003).
L. Medlin, H. Elwood, S. Stickel and M. Sogin, Gene 7, 491–499 (1988).
D. Oldach, C. Delwiche, K. Jakobsen, T. Tengs, E. Brown, J. Kempton, E. Schaefer, H. Bowers, H. Glasgow, J. Burkholder, K. Steidinger and P. Rublee, Proc. Natl. Acad. Sci. 97, 4303–4308 (2000).
P. Rublee, J. Kempton, E. Schaefer, J. Burkholder, H. Glasgow, and D. Oldach, Va. J. Sci. 50, 325–335 (1999).
J. Saldarriaga, F. Taylor, P. Keeling and T. Cavalier-Smith, J. Mol. Evol. 53, 204–213 (2001).
M. Sogin, in: PCR protocols: a guide to methods and applications, M. Innis, D. Gelfand, J. Sninsky and T. White, eds. (Academic Press, San Diego), pp. 307–314 (1990).
A. Sournia, Atlas du phytoplancton marin, (Editions du Centre National de la Recherche Scientifique, Paris) 219 pp. (1986).
K. Steidinger and K. Tangen, in: Identifying Marine Plankton, C. Tomas, ed. (Academic Press, New York), pp. 387–584 (1997).

Linking Population and Physiological Diversity in *Karenia brevis* from the Texas Coast

L. Campbell,[1] J. M. Ivy,[2] P. Loret,[3] T. A. Villareal,[4] Kelly Soltysiak,[1] and J. R. Gold[5]

[1]*Department of Oceanography, Texas A&M University, College Station, TX 77843, USA;* [2]*Department of Biology, Texas A&M University;* [3]*Université du Maine, Faculté des Sciences, 72085 Le Mans Cedex 9, France;* [4]*Marine Science Institute, University of Texas–Austin, Port Aransas, TX 78373, USA;* [5]*Deptartment of Wildlife and Fisheries Sciences, Texas A&M University.*

Abstract

Blooms of the toxic dinoflagellate *Karenia brevis* along the Texas coast are increasing in frequency, yet the source population and specific factors influencing bloom initiation and intensity are poorly known. Significant differences in growth rates and toxin production were observed among clonal isolates from a 1999 bloom when grown under identical conditions. This may reflect genetic diversity that serves as a repository from which different subpopulations bloom in response to appropriate environmental conditions. To test this hypothesis, hypervariable genetic markers known as microsatellites (msats) are being developed to examine genetic diversity among populations of *K. brevis.* PCR amplification of two msat loci from genomic DNA of Texas *K. brevis* clones demonstrated different allele constitutions among these clones. In addition, msat markers appear to be useful fingerprinting tools for differentiating *K. brevis* and *K. mikimotoi.* The correlation between differences in microsatellite genotypes and growth rate and toxin production clearly demonstrates the utility of combining genetic and physiological approaches.

Introduction

The source population for *Karenia brevis* blooms and specific factors influencing bloom intensity are poorly understood in the western Gulf of Mexico. Previous results suggested a high level of genetic diversity exists within populations of *K. brevis* (Baden and Tomas, 1988; Magaña, 2001; Loret *et al.,* 2002). When maintained under identical conditions, the growth rate of *K. brevis* clone SP1 was twofold higher than SP2 and its cellular toxin concentration was threefold lower (Loret *et al.,* 2002). This genetic variability may serve as a repository from which different subpopulations bloom in response to appropriate environmental conditions. Such diversity emphasizes the need for new hypervariable genetic markers, such as microsatellites, which can be utilized in population- and species-level studies of harmful algal blooms. The objectives of our research were to: (1) establish clonal cultures of *Karenia* from bloom events along the Texas coast; (2) examine differences in growth rates among clonal isolates; and (3) identify microsatellite loci and develop PCR primers for genotyping analysis. Establishing links between allelic profiles and physiological properties will yield insight into population-level responses of *K. brevis* to changes in environmental variables. Ultimately, this information can be used to predict responses of *K. brevis* at the population level to environmental changes and to assess how these responses affect and influence bloom formation and dynamics.

Materials and Methods

Cultures Clonal cultures of *K. brevis* were established from samples collected during a fall 1999 bloom, and clones of *K. mikimotoi* were established from a winter 2002 bloom. Single cells were picked out using micropipettes under a stereomicroscope and transferred to wells in a microtiter plate containing "L1"/10 medium (Guillard and Hargraves, 1993). Once established, replicate clonal cultures were maintained in L1 medium made with either low salinity (29 PSU) or high salinity (36 PSU) filtered sea water and grown on a 12:12 light:dark cycle.

Growth Rates Experiments (performed in triplicate) were conducted with cultures acclimated to two light levels (71 and 100 $\mu E\ m^{-2}s^{-1}$), and for selected clones, at both 29 and 36 PSU, at 20°C. Growth rates were determined from daily measurements of *in vivo* fluorescence (Brand *et al.,* 1981). Fluorescence measurements were validated with cell counts.

Microsatellite Development Genomic DNA libraries of DNA fragments of *K. brevis* SP2 (300–500 base pairs in size) were constructed via an approach for producing "enriched"

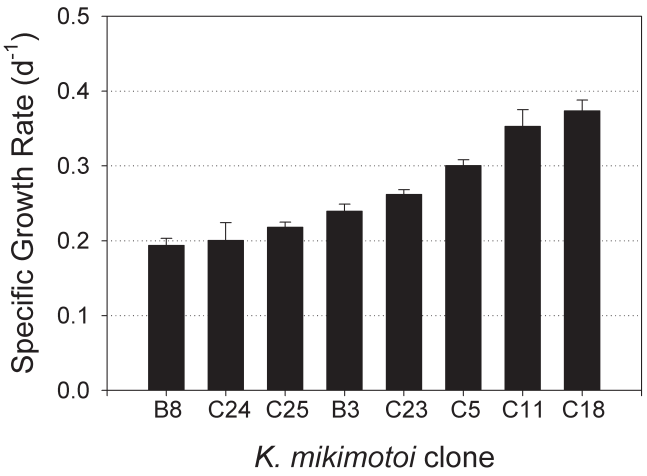

Figure 1 Specific growth rates of eight *K. mikimotoi* clones isolated from a coastal Texas bloom in 2002. A ~twofold range in growth rates was observed among the clones when grown at 20°C in L1 medium (29 PSU) under 71 $\mu Ein\ m^{-2}\ s^{-1}$. Growth rates of clones B8, C24, C25, and B3 are significantly different from C23, C5, C11 and C18 (t-test, $P < 0.05$). Error bars are ± 1 SD in all figures.

Steidinger, K. A., J. H. Landsberg, C. R. Tomas, and G. A. Vargo (Eds.). 2004. Harmful Algae 2002. Florida Fish and Wildlife Conservation Commission, Florida Institute of Oceanography, and Intergovernmental Oceanographic Commission of UNESCO.

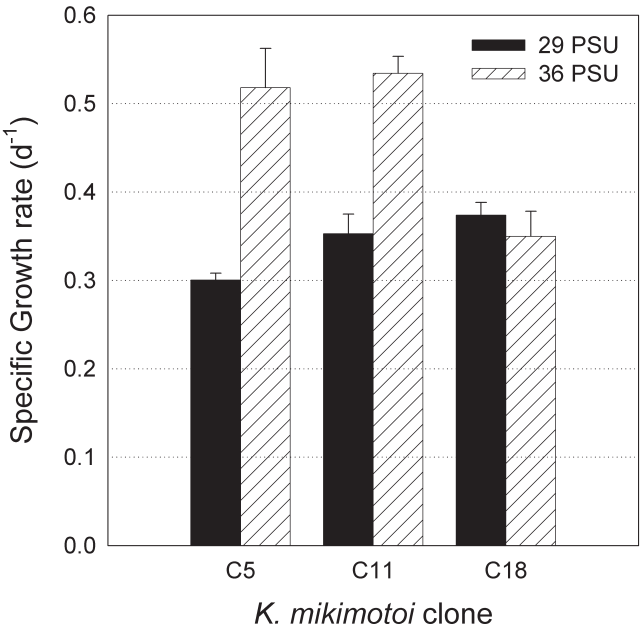

Figure 2 Comparison of specific growth rates among three *K. mikimotoi* clones grown at 20°C, 71 µEin $m^{-2\ s-1}$ at low and high salinities. For C5 and C11, growth rates were significantly different at the two salinities (t-test, $P < 0.05$).

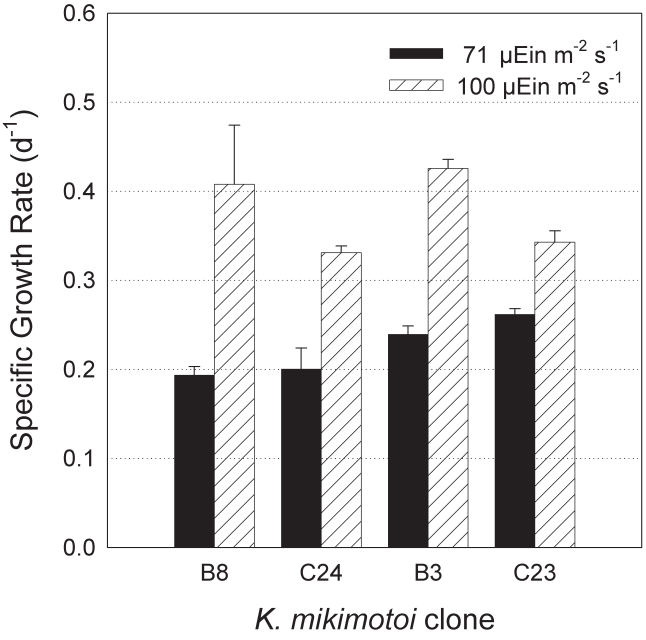

Figure 3 Variability in specific growth rates among *K. mikimotoi* clones grown at 20°C, in 29 PSU L1 medium at two light intensities.

msat libraries (Walbieser, 1994; Connell *et al.,* 1998; A. Pepper, pers. comm.). Biotinylated probes (containing desired repeat motifs [$(TA)_{30}$, $(CA)_{20}$, $(GA)_{20}$, $(TGA)_{15}$, $(ACA)_{15}$]) annealed to genomic fragments were bound to streptavidin-coated paramagnetic particles that held the complexes in place; non-bound genomic fragments that lacked repeat motifs were washed away. The bound fragments were then chemically released and cloned into "enriched" libraries. The enriched libraries contained a high percentage of msats, thereby increasing efficiency of screening. Approximately 200 clones from the library were sequenced. Primers were designed to genomic DNA flanking candidate msat loci using OLIGO™ (ver. 5.0, NBI, Plymouth, MN). PCR amplifications were performed in 10 µL reactions using ExTaq™

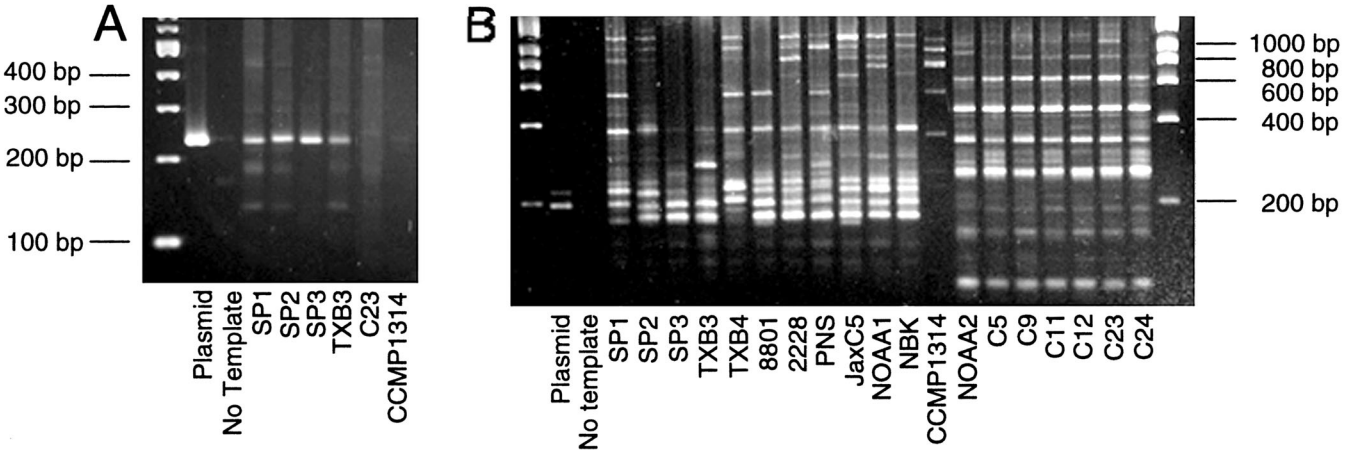

Figure 4 PCR-amplified products for msat loci *KB3* and *KB5.* **A** PCR amplification of msat *KB3* for Texas *K. brevis* clones from the 1999 bloom (SP1, SP2, SP3,TXB3), *K. mikimotoi* clone C23 from the 2002 bloom, and *Amphidinium carterae* (CCMP1314); *KB3* plasmid DNA from SP2 library as positive control, no template as a negative control; 100 bp ladder; *KB3*-forward primer: CGTGACTCAGAGTGGCAAATGG; *KB3* reverse primer: AACATGGCTGATCAACTCAACACC; 2% Metaphore agarose gel; **B** As in (A) for msat *KB5* with additional *K. brevis* 1999 clone (TXB4) and historical clones: 8801 (B. Richardson), NBK (C. Hyatt), CCMP2228, and PNS, JaxC5, NOAA1 (G. Doucette); *K. mikimotoi* clones NOAA2 (S. Morton) and C5–C24 (2002 TX bloom); *KB5* forward primer: ATCCAGGTCGTCCATTCAAGTC; *KB5* reverse primer: CGAAACGCCGGTTCTCTTC; 200 bp ladder.

polymerase and standard conditions as suggested by the manufacturer (Takara) and following a touchdown PCR protocol (Don *et al.,* 1991).

Results and Discussion

Five clonal cultures of *K. brevis* were established from a Texas coastal bloom off Brownsville in fall 1999: SP1, SP2, SP3, TXB3, TXB4 (Loret *et al.,* 2002; Magaña, 2001; B. Richardson, pers. comm.). Twenty-two clonal cultures of *K. mikimotoi* were established from a bloom in Corpus Christi Bay in January 2002. Internal transcribed spacer (ITS) and large subunit (LSU) rRNA sequences for the clonal isolates confirmed the species identifications.

Initial experiments with eight *K. mikimotoi* clones demonstrated significant differences among growth rates when cultures were grown under identical conditions (t-test; $P < 0.05$; Figs. 1–3). Observed variations in growth rates for strains grown at the different salinities and light levels suggest these are genetically distinct clones (Fig. 2 and 3). The almost-twofold range in growth rate among *K. mikimotoi* clones (Fig. 1) is similar to our previous findings for *K. brevis* clones (Loret *et al.,* 2002) and for other phytoplankton species (*e.g., Pseudo-nitzschia australis* and *P. multiseries;* Kudela *et al.,* this Proceedings).

Hypervariable molecular markers (msats) are being developed to determine profiles of genetic and ecological diversity of *Karenia* populations. Ten candidate msat loci have been identified. Examination of PCR products for two loci, *KB3* and *KB5,* demonstrated different sizes and banding patterns among the *K. brevis* clones from Texas and Florida (Fig. 4). Small size differences at locus *KB3* were noted among the *K. brevis* clones from the 1999 bloom (Fig. 4A), and sequencing results confirmed that the msat varied in number of GTT repeats among clones. Locus KB5 is a complex microsatellite and preliminary results indicate that this marker may be useful for fingerprinting (Fig. 4B). The capability to differentiate both between and among individual *K. brevis* and *K. mikimotoi* clones is a valuable tool. The correlation between differences in microsatellite genotype and physiology (*e.g.,* SP1 vs. SP2) demonstrates the utility of combining genetic and physiological approaches.

Further study of the extent of diversity in physiological properties and toxin production among *Karenia* isolates, together with genetic profiles, is necessary to develop realistic predictive models of bloom dynamics and to assess potential toxicity. By establishing links between allelic profiles and physiological properties, models can ultimately be employed to forecast the response of *K. brevis* at the population level to changes in environmental variables. With a better understanding of the responses of different genotypes, we can better predict variability in both spatial and temporal bloom dynamics.

Acknowledgements

We thank D. Arreola for technical assistance and acknowledge the helpful advice from A. Pepper, Department of Biology, TAMU. This research is funded by awards to L.C. and J.R.G. from the EPA's Science to Achieve Results (STAR) Program #R-83041301-0 and the Interdisciplinary Research Program at Texas A&M University.

References

D. G. Baden and C. R. Tomas, Toxicon 26, 961–963 (1988).
L. E. Brand, L. S. Murphy, R. R. L. Guillard and H. T. Lee, Mar. Biol. 62, 103–110 (1981).
J. P. Connell, S. Pammi, M. J. Iqbal, T. Huizinga and A. S. Reddy, Plant Mol. Biol. Rep. 16, 341–349 (1998).
R. H. Don, P. T. Cox, B. J. Wainwright, K. Baker and J. S. Mattick, Nucl. Acids Res. 19, 4008 (1991).
R. R. L. Guillard and P. E. Hargraves, Phycologia 32, 234–236 (1993).
R. Kudela, A. Roberts, and M. Armstrong, this Proceedings.
P. Loret, T. Tengs, T. A. Villareal, H. Singler, B. Richardson, P. McGuire, S. Morton, M. Busman and L. Campbell, J. Plankton Res. 24, 735–739 (2002).
H. A. Magaña, M.S. Thesis, Texas A&M University Corpus Christi, 1–86 (2001).
G. C. Walbieser, BioTechniques 19, 742–744 (1994).

Differentiating Two Florida Harmful Algal Bloom Species Using HPLC Pigment Characterization

Bradley A. Pederson[1], Gary J. Kirkpatrick[1], Allison J. Haywood[2], Barbara A. Berg[1], and Christopher J. Higham[1]
[1]*Mote Marine Laboratory, 1600 Ken Thompson Pkwy., Sarasota, FL 34236, USA;*
[2]*Florida Marine Research Institute, St. Petersburg, FL, USA; Cawthron Institute, Nelson, New Zealand*

Abstract

A large scale bloom of *Karenia brevis* was identified on the west Florida continental shelf during the ECOHAB process cruise conducted September 20–25, 2001. Offshore of the large bloom, a small isolated patch of morphologically distinct *K. brevis*-like cells was also found. The inshore and offshore bloom locations were analyzed for algal pigment content. Results indicate that the offshore patch was distinct in relation to the gyroxanthin-diester to chlorophyll *a* ratio as well as the amount of fucoxanthin per cell. Bloom data from previous years have shown the gyroxanthin-diester/chl *a* ratio to be constant for *Karenia brevis,* and studies comparing multiple *Karenia* species demonstrated a variation in both gyroxanthin-diester/chl *a* and fucoxanthin per cell. The distinct pigment signature coupled with the morphological differences observed microscopically suggest the offshore patch may have been comprised of a *Karenia* species other than *K. brevis.*

Introduction

The algal photopigment gyroxanthin-diester has been previously shown to be a good marker pigment for the harmful algal bloom species *Karenia brevis* (Millie *et al.,* 1995; unpublished data). *Karenia brevis* is a dinoflagellate that also contains fucoxanthin and lacks peridinin. The unique pigment signature of *K. brevis* lends itself well to discrimination by chemotaxonomic methods allowing *K. brevis* to be distinguished from other algae using High Performance Liquid Chromatography (HPLC) analyses. The ratio of gyroxanthin-diester to chlorophyll *a* (here after referred to as gyro:chl *a*) in both natural populations and cultures of *K. brevis* has also been shown to be constant (~0.04) (Millie *et al.,* 1995; Higham *et al.,* 2002; unpublished data), providing a means to distinguish between various gyroxanthin-diester containing dinoflagellates (Kirkpatrick *et al.,* 2000).

A large bloom of *K. brevis* was found on the west Florida continental shelf during the 2001 ECOHAB:Florida Process cruise (September 20–25, 2001). Within this area, shipboard analyses identified an isolated patch of *K. brevis*-like cells about 100 km offshore. Microscopic evaluation of the offshore patch qualitatively identified *K. brevis*-like cells which appeared morphologically distinct from the inshore bloom, raising the question as to whether the cells were *K. brevis,* a distinct clone of *K. brevis* or a different species of *Karenia.* Since cruise and culture data have consistantly shown a gyroxanthin-diester:chlorophyll *a* ratio of ~0.04, a comparison of the pigment contents for the inshore and offshore patches should provide information pertaining to whether the offshore bloom was *K. brevis* or not.

Materials and Methods

The field portion of this study was conducted during a cruise on the west Florida continental shelf onboard the R.V. *Suncoaster* (September 20–25, 2001). Sampling stations were established inside and outside of the bloom patches of *K. brevis.* At each station, hydrographic profiles of the water column were measured with a Sea Bird SBE 25 CTD profiling system. Niskin bottles, cast to selected depths, were used to collect water for assessment of phytoplankton.

Phytoplankton biomass was enumerated both microscopically and by algal pigments derived using HPLC (Wright, 1996). For shipboard microscopic enumeration, sample aliquots were preserved at time of sampling with Utermöhl's solution and concentrated and enumerated using an inverted microscope (after Lund *et al.,* 1958). For photopigment analyses, aliquots of water were drawn under low vacuum onto GF/F glass-fiber filters and immediately frozen and stored in liquid nitrogen. HPLC pigment analyses followed the methodology of Wright *et al.* (1991). Pigment peaks were identified and quantified at 440 nm by comparison of retention times and absorption spectra to those of authentic standards using a Shimadzu SPD-10A HPLC system. Chlorophyll and carotenoid pigment ratios, based on published chlorophyll *a*:diagnostic pigment ratios within the representative phylogenetic groups (Wright *et al.,* 1996), were used to correct final gyro:chl *a* ratios for the presence of dinoflagellates and cyanophytes.

Results

Data were divided into two groups, a group of inshore stations and a group from the offshore patch. Only inshore stations with cell abundances over 10^6 cells liter^{-1} with cellular chlorophyll *a* contents between 5.0 and 8.0 pg cell^{-1} were chosen in an attempt to minimize the contribution of other algae to total pigment values and to normalize for light history. The offshore patch was represented by data collected approximately 90 to 100 km offshore. Average values of pigment per cell from both the inshore and offshore patches are listed in Table 1. Total chlorophyll *a* at each station was also corrected for the contribution of other organisms using ratios of chlorophyll *a* to zeaxanthin and peridinin. Although gyroxanthin-diester per cell was not significantly different between patches, cellular fucoxanthin and the corrected gyro:chl *a* ratio were.

A comparison of pigment data from the 2001 cruise with those from cultures of other gyroxanthin-diester con-

Steidinger, K. A., J. H. Landsberg, C. R. Tomas, and G. A. Vargo (Eds.). 2004. Harmful Algae 2002. Florida Fish and Wildlife Conservation Commission, Florida Institute of Oceanography, and Intergovernmental Oceanographic Commission of UNESCO.

Table 1 Average pigment content per *K. brevis* cell (pg L^{-1}). Italics indicate significant differences according to the t-test.

	Stations >10^6 cells L^{-1}	Std. Dev.	Station 27	Std. Dev.	T Test
chlorophyll *c3*	0.502	0.186	0.379	0.017	0.169
chlorophyll *c1+c2*	1.135	0.295	0.870	0.046	0.081
peridinin	*0.106*	0.043	*0.021*	0.003	*0.004*
19'-butanoyloxyfucoxanthin	*0.394*	0.113	*0.559*	0.032	*0.019*
fucoxanthin	*1.195*	0.263	*0.155*	0.003	*0.000*
9'-cis-neoxanthin	0.010	0.011	0.000	0.000	0.080
19'-hexanoyloxyfucoxanthin	0.553	0.157	0.728	0.052	0.057
violaxanthin	0.000	0.000	0.000	0.000	
diadinoxanthin	*0.874*	0.356	*1.548*	0.096	*0.006*
antheraxanthin	0.014	0.012	0.014	0.009	0.958
alloxanthin	*0.040*	0.006	*0.024*	0.005	*0.048*
diatoxanthin	*0.066*	0.028	*0.221*	0.016	*0.001*
lutein	0.000	0.000	0.000	0.000	
zeaxanthin	*0.051*	0.030	*0.186*	0.014	*0.001*
gyroxanthin-diester	0.253	0.064	0.195	0.015	0.086
chlorophyll *b*	0.031	0.011	0.029	0.002	0.803
chlorophyll *a*	6.339	0.932	6.380	0.490	0.941
corrected chlorophyll *a*	6.098	0.902	5.840	0.455	0.627
corrected gyro:chl *a*	*0.041*	0.007	*0.033*	0.000	*0.034*

taining dinoflagellates showed that the inshore stations matched well with pigment contents expected for *K. brevis* (Table 2). The offshore patch did not. Although the cellular gyroxanthin-diester and fucoxanthin contents for the inshore *K. brevis* bloom were lower than those found in culture, the gyro:chl *a* ratios are very similar. The cellular fucoxanthin, gyroxanthin-diester and gyro:chl *a* for the offshore patch were all lower than *K. brevis* and the other gyroxanthin-diester containing dinoflagellates.

Table 2 Comparison of cellular pigment content (pg $cell^{-1}$) for the gyroxanthin-diester containing dinoflagellates *Karenia mikimotoi* (NZ), *K. mikimotoi* (Japan), *K. brevis* (USA), *Karlodinium micrum, Karenia selliformis, K. bidigitata* and *K. papilionacea.* Data are from laboratory cultures (table presented at the IX annual HAB conference in Tasmania, courtesy of Dr. Allison Haywood and Dr. Gary Kirkpatrick).

Pigment	*K. mikimotoi* (NZ)	*K. mikimotoi* (Japan)	*K. brevis* (USA)	*K. micrum*	*K. selliformis*	*K. bidigitata*	*K. papilionacea*
chlorophyll *c3*	0.35	0.38	0.65	0.16	0.31	0.24	1.18
chlorophyll *c1&c2*	0.74	1.03	1.34	0.44	0.66	0.62	2.64
peridinin	0.00	0.00	0.00	0.00	0.00	0.00	0.00
19'-butanoyloxyfucoxanthin	0.39	0.79	1.20	0.24	0.43	0.79	1.17
fucoxanthin	*1.53*	*0.91*	*2.06*	*0.20*	*0.02*	*0.02*	*3.58*
9'-cis-neoxanthin	0.00	0.00	0.00	0.00	0.00	0.00	0.00
19'-hexanoyloxyfucoxanthin	0.85	1.60	1.29	0.88	1.27	1.61	3.89
violaxanthin	0.02	0.11	0.04	0.00	0.00	0.02	0.05
diadinoxanthin	0.22	0.24	1.18	0.13	0.24	0.24	0.85
antheraxanthin	0.00	0.01	0.02	0.01	0.00	0.00	0.03
alloxanthin	0.01	0.03	0.00	0.02	0.01	0.00	0.03
diatoxanthin	0.14	0.27	0.22	0.31	0.02	0.10	0.18
lutein	0.00	0.00	0.00	0.00	0.00	0.00	0.00
zeaxanthin	0.03	0.01	0.02	0.01	0.03	0.02	0.09
gyroxanthin-diester	*0.17*	*0.31*	*0.32*	*0.12*	*0.20*	*0.14*	*0.67*
chlorophyll *b*	0.00	0.00	0.00	0.00	0.00	0.00	0.00
chlorophyll *a*	3.08	3.72	7.26	1.26	3.29	2.66	12.04
gyro:chlorophyll *a*	*0.055*	*0.083*	*0.044*	*0.095*	*0.061*	*0.053*	*0.056*

Discussion

The pigment signature of the offshore patch indicates it was not *Karenia brevis*. The ratio of gyro:chl *a* for *K. brevis* is consistantly 0.04 (±0.007, for these data, ±0.00 from culture data of Higham *et al.,* 2002), and the offshore patch was distinct in relation to fucoxanthin per cell as well as the gyro:chl *a* ratio. These values do not seem to match any of the gyroxanthin-diester containing dinoflagellates listed in Table 2.

The differences in pigment content between the inshore and offshore blooms seem to be related to light acclimation. Based on the fucoxanthin and diadinoxanthin/diatoxanthin content, the inshore patch appeared to be shade-adapted while the offshore patch was acclimated to higher light conditions. Values of the accessory pigment fucoxanthin were higher inshore while the photoprotective pigments, diadinoxanthin and diatoxanthin, were lower. Relative fluorescence values were also an order of magnitude higher inshore (~4.3 μg L^{-1} inshore, ~0.6 μg L^{-1} offshore). The pigment content per cell coupled with the presence of more *in-situ* chlorophyll *a* suggests light levels were lower within the inshore patch. Photo-acclimation may account for the differences in pigment contents per cell but not the difference in the gyro:chl *a* ratio, since it is constant regardless of light history.

The gyro:chl *a* ratio for the offshore patch was significantly lower than that of the inshore *K. brevis* bloom. Coupled with the subtle qualitative morphologic differences observed onboard ship and the consistant gyro:chl *a* ratio of 0.04 for *K. brevis,* it seems likely that the offshore patch was a *Karenia* species other than *K. brevis.*

Acknowledgements

Funding for this work was provided by ECOHAB: Florida (NOAA and US EPA) and the Florida Marine Research Institute. The authors would like to thank the crews of the R/V *Suncoaster* (Florida Institute of Oceanography).

References

C. Higham, G. J. Kirkpatrick, B. A. Pederson and B. A. Berg, this Proceedings.

G. J. Kirkpatrick, A. J. Haywood and J Adamson, presented during the IXth International Conference on Harmful Algae, Hobart, Tasmania, Australia (February 2000).

J. W. G. Lund, C. Kipling and E. D. LeCren, Hydrobiologia 11, 143–170 (1958).

M. D. Mackey, H. W. Higgins, D. J. Mackey and D. Holdsworth, Deep-Sea Res. 45, 1441–1468 (1998).

D. F. Millie, G. J. Kirkpatrick and B. T. Vinyard, Mar. Ecol. Prog. Ser. 120, 65–75 (1995).

S. W. Wright, S. Jeffrey, R. Mantoura, C. Llewellyn, C. Bjornland, D. Repeta, and N. Welschmeyer, Mar. Ecol. Prog. Ser. 77: 183–196 (1991).

S. W. Wright, D. P. Thomas, H. J. Marchant, H. W. Higgins, M. D. Mackey and D. J. Mackey, Mar. Ecol. Prog. Ser. 144, 285–298 (1996).

Molecular Analysis of *Pfiesteria piscicida* Life Cycle Stages Using Nuclear Staining Techniques and Whole Cell *in Situ* Hybridization with Peptide Nucleic Acid Probes

Mark W. Vandersea, R. Wayne Litaker, Steven R. Kibler, and Patricia A. Tester
Center for Coastal Fisheries and Habitat Research, National Ocean Service, NOAA,
101 Pivers Island Road, Beaufort, NC 28516-9722, USA

Abstract

Elucidating dinoflagellate life cycles can be difficult. We describe the application of nuclear staining techniques and peptide nucleic acid (PNA) probes to investigate life cycle stages of *Pfiesteria piscicida.* PNAs are synthetic molecules that mimic DNA, but have a neutral peptide backbone rather than the charged sugar-phosphate backbone found in DNA. The neutral charge allows PNAs to penetrate cells more easily and to hybridize with DNA or RNA target sequences more strongly than conventional oligonucleotide DNA probes. In this study, samples from *P. piscicida* cultures raised on *Rhodomonas* sp. and from aquaria containing a diverse population of eukaryotic species were processed for nuclear staining with DAPI and *in situ* hybridization with species-specific PNA probes. Comparative analysis of individual cells with epifluorescent and brightfield optics allowed cellular morphologies and nuclear characteristics to be associated with specific life cycle stages. The nuclear staining and PNA probe technologies we describe represent an excellent set of "molecular tools" that may be useful for identifying life cycle stages of other phytoplankton species even in complex natural assemblages.

Introduction

Free-living, marine dinoflagellates are typified by a well-defined, haplontic life cycle with relatively few stages. The most unusual departure from this life cycle is one reported for the heterotrophic dinoflagellate *Pfiesteria piscicida* Steidinger et Burkholder. We established clonal cultures of *P. piscicida* (Litaker *et al.,* 1999) and failed to observe any life cycle stage that was atypical of a free-living, marine dinoflagellate. This prompted a rigorous study to resolve the life cycle of *P. piscicida* using a number of techniques including nuclear staining combined with traditional light microscopy, and *in situ* hybridization with fluorescently labeled species-specific peptide nucleic acid (PNA) probes. Nuclear staining enabled us to document mitotic and meiotic events during *P. piscicida*'s cell cycle. Fluorescent *in situ* hybridization techniques facilitated unambiguous identification of life cycle stage transitions. This paper describes methods we employed to elucidate the life cycle of *P. piscicida*.

Materials and Methods

Nuclear Staining and Visualization *Pfiesteria piscicida* cells were fixed and permeabilized by mixing 50% glutaraldehyde and Triton X-100™ to make a solution with the final concentration of 1% for both reagents. Hoechst 33258 or DAPI (Sigma) was added to the fixed samples to attain a final dye concentration of 100 to 500 ng · mL^{-1}. These two fluorochromes were utilized interchangeably, as they have similar excitation and emission spectra (Green 1990). After addition of the stain, cell samples were microwaved at a full power setting (1100 W) for 0.5 sec · mL^{-1} of cell sample to achieve greater dye penetration. Concentrated 20 µL aliquots of labeled cells were allowed to bind to glass slides coated with 0.01% poly-L-lysine (Sigma) and then viewed with brightfield and epifluorescent microscopy.

The extreme impermeability of hypnocysts required a different staining procedure. Fixed hypnocysts were transferred to poly-L-lysine-coated slides and allowed to dry completely. The slides were alternately rinsed with 95% ethanol and de-ionized water to permeabilize the cysts and remove precipitated salt. DAPI or Hoechst 33258 was then added directly to the samples on the slides (300–500 ng · mL^{-1} final conc.) before a cover slip was placed on the slide and samples were examined with brightfield and epifluorescent microscopy (λ_{ex}=350 nm, λ_{em}=480 nm). The Metamorph™ software package was used to overlay epifluorescent micrographs with brightfield images. This allowed specific morphological changes and cellular characteristics to be associated with the nuclear changes occurring in the cells.

Whole Cell* in Situ *Hybridization Cy5 conjugated, PNA probes were utilized in these studies (Boston Probes, Inc.). Three separate small subunit rRNA (SSU rRNA) antisense PNA probes were designed and synthesized. The first probe was specific for *P. piscicida;* the second was a universal eukaryote-specific probe. The eukaryote probe was used as a positive control probe to ensure that negative probing results were not due to a failure of the PNA to enter a particular cell. The third probe was a universal eubacteria-specific probe, which served as a negative control probe to assess non-specific hybridization (Litaker *et al.,* 2002).

Whole-cell probing was performed using reagents, filter apparati, and methods established by Miller and Scholin (1998, 2000). Aliquots of live cells from *P. piscicida* cultures feeding on either algae or fish were vacuum-filtered onto 13 mm, 0.2 µm polycarbonate membrane filters and fixed with 5 mL of saline ethanol for 1.5 hr at room temperature. The saline ethanol fixative consisted of 44 mL 95% ethanol, 10 mL de-ionized H_2O and 6 mL of 25× SET buffer (3.75 M NaCl, 25 mM EDTA, 0.5 M Tris HCl; pH 7.8). After fixation, the cells were filtered once more and rinsed for 20 min with 1 mL of hybridization buffer {5× SET, 0.1% (v/v) IGEPAL-CA630 (Sigma), 25 µg · mL^{-1} polyadenylic acid

Steidinger, K. A., J. H. Landsberg, C. R. Tomas, and G. A. Vargo (Eds.). 2004. Harmful Algae 2002. Florida Fish and Wildlife Conservation Commission, Florida Institute of Oceanography, and Intergovernmental Oceanographic Commission of UNESCO.

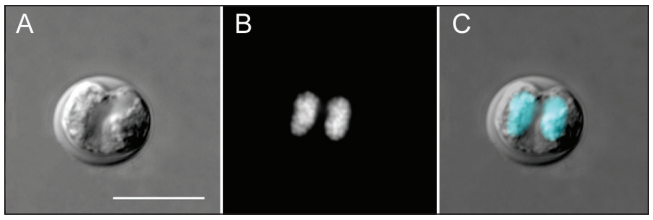

Figure 1 **A** *Pfiesteria piscicida* division cyst. **B** Epifluorescent image of the DAPI stained nuclei. **C** The epifluorescent nuclei (false colored blue) were superimposed on the light micrograph to show the position of the nuclei within the cell. Scale bar = 10 μM.

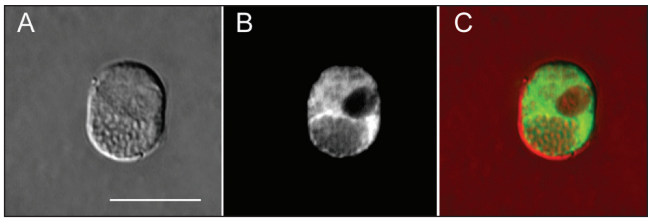

Figure 2 **A** *Pfiesteria piscicida* dinospore hybridized with a *P. piscicida*-specific PNA probe. **B** Epifluorescent image showing where the probe specifically hybridized with the rRNA in the cell. **C** The epifluorescent image (false colored green) was superimposed on the light micrograph to demonstrate the spatial relationship of the rRNA within the dinospore. Scale bar = 10 μM.

(Sigma)}. Next, the ethanol saline solution was removed by filtration. The cells were then resuspended in 0.5 mL of hybridization buffer containing 0.25 μM of either the *P. piscicida*-specific, the universal eukaryote probe, or the universal eubacteria probe. "No probe" control cells were resuspended with 0.5 mL of hybridization buffer. All samples were incubated at 55°C for 1hr and then filtered and rinsed with 1 mL of pre-warmed (55°C) 5× SET buffer. The filter membranes were placed cell-side down onto poly-L-lysine-coated microscope slides. The filter membranes were then peeled away, leaving a large percentage of the cells adhering to the slide surface. One drop of Slowfade™ Light Antifade solution (Molecular Probes, OR) was placed on each cell sample. Samples were then overlain with a cover slip and analyzed using brightfield and Cy5 epifluorescence microscopy (λ_{ex} = 590–650 nm, λ_{em} = 662–738 nm, dichroic LP beamsplitter 660 nm). Camera settings for each epifluorescent image of the experimental groups were held constant so that comparative analyses of relative fluorescence intensity could be made between probed and non-probed cells.

Results and Discussion

The microwave staining technique described above enabled the nuclear stains to penetrate most life cycle stages and yielded consistent and reproducible fluorescent staining (Fig.1). The only exception was the thick-walled hypnocyst stage. Hypnocyst staining was attained by allowing concentrated aliquots of cells to completely dry on poly-L-lysine-coated microscope slides, followed by alternating gentle rinsing with 95% ethanol and de-ionized water to permeabilize the cysts and remove precipitated salt. The DAPI or Hoechst stain was added to the cells directly on the slide. Combining the nuclear staining results with time-lapse video microscopy observations made it possible to correlate sexual and asexual life cycle stages with specific nuclear changes (Litaker *et al.,* 2002). For example, mitosis as indicated by typical anaphase and early telophase nuclear morphologies was only observed in division cysts (Fig. 1). In contrast, none of more than 1500 DAPI-stained, free-swimming "mastigote" or "dinospore" cells from a rapidly dividing population (1×10^4 cells · mL^{-1}) were binucleate or contained characteristic anaphase nuclear signatures. This indicated that binary fission of free-swimming cells does not occur in the water column.

PNA probes were successfully used to identify the life cycle stages of *P. piscicida* (fig. 2, Litaker *et al.,* 2002). *P. piscicida* cells grown in culture were first tested with the *P. piscicida*-specific probe to verify that all cell stages were permeable and hybridized with the probe. Next, we attempted to hybridize the *P. piscicida* probe with other *Pfiesteria* like dinoflagellates to assess the possible cross reactivity of the probe (fig. 16, Litaker *et al.,* 2002). There was no cross-reactivity with the dinoflagellates that we tested. A battery of experimental controls consisting of a universal eukaryote probe (positive control), a universal eubacteria probe (negative control), and a "no probe control" (evaluates autofluorescence) insured that hybridization results obtained from a multi-species sample would be valid. Finally, samples from *P. piscicida* cultures raised separately on algae and fish were hybridized with the suite of PNA probes. All hybridization positive cells were imaged and recorded and a census of life cycle stages was constructed. An image of a hybridization-positive dinospore (Fig. 2) demonstrates the reticulate rRNA labeling pattern that served as an important criterion for assessing a hybridization positive cell. Direct observations of these probed samples indicated that only life cycle stages typical of free-living marine dinoflagellates were hybridization-positive for the *P. piscicida*-specific probe. Detailed results and analyses of our *in situ* hybridization studies are illustrated in Litaker *et al.,* 2002.

Correctly using PNA probes requires an understanding of their strengths and weaknesses. The neutral backbone of PNA probes allows them to penetrate cells more easily than DNA oligonucleotide probes, which carry a net negative charge. PNAs also bind more tightly, and 50,000× faster to their corresponding DNA or RNA targets than do analogous DNA probes (Carlsson *et al.,* 1996, Demers *et al.,* 2001). These properties make PNAs ideal for *in situ* hybridization studies. However, one limitation of PNA probes is that they have a higher melting temperature. Consequently, the probes must be shorter (14–18 bp) to stay within a 50°–60°C hybridization temperature. In contrast, a typical olignonucleotide probe is 18–20 bp. This means that there is a greater possibility of non-specific hybridization

with PNAs than with oligonucleotide probes. Therefore, it is extremely important to test PNA probes for potential cross-reactivity problems.

The results of our experiments showed that *P. piscicida* has a normal haplontic dinoflagellate life cycle typical of free-living marine dinoflagellates. The combination of nuclear staining techniques, careful observation of cells with high-resolution microscopy and time-lapse video microscopy, and whole-cell *in situ* hybridization identified *P. piscicida* life cycle stages and stage transformations. The experimental design included rigorous positive and negative controls that are necessary for any life cycle study that employs these research techniques. Finally, in certain cases, PNA probes may offer advantages over oligonuleotide probes and should have potential use in a broad spectrum of phytoplankton research.

References

C. Carlsson, M. Jonsson, B. Norden, M. T. Dulay, R. N. Zare, J Noolandi, P. E. Nielsen, L.-C. Tsui and J. Zielenski, Nature 380, 207 (1996).

D. B. Demers, E. T. Curry and A. C. Sozer, Am. J. Hum. Gen. 57, 120 (1995).

F. J. Green, in: The Sigma-Aldrich Handbook of Stains, Dyes, and Indicators (Aldrich Chemical, Wisconsin), pp. 244 (1990).

P. E. Miller and C. A. Scholin, J. Phycol. 34, 371–382 (1998).

P. E. Miller and C. A. Scholin, J. Phycol. 36, 238–250 (2000).

R. W. Litaker, P. A. Tester, A. Colorni, M. G. Levy and E. J. Noga, J. Phycol. 35, 1379–1389 (1999).

R. W. Litaker, M. W. Vandersea, S. R. Kibler, V. J. Madden, E. J. Noga and P. A. Tester, J. Phycol. 38, 442–463 (2002).

Morphology of *Fibrocapsa japonica* Cysts Formed under Laboratory Conditions

M. Karin de Boer, Marion van Rijssel, and Engel G. Vrieling
Department of Marine Biology, Center for Ecological and Evolutionary Studies, University of Groningen, PO Box 14, 9750 AA Haren, the Netherlands

Abstract

Cysts of *Fibrocapsa japonica* Toriumi and Takano were reported once in field samples from Japan but were never observed under laboratory conditions. In this study we followed a similar procedure used for *Chattonella* sp. to induce cyst formation in recently isolated *F. japonica* strains from Dutch coastal waters. After 9 months in the dark, a biofilm was formed, which had an evenly distributed polymer network. In these biofilms, a few cysts were found in cultures incubated at 5.5°C. Size and form of the cysts appeared to be similar to natural cysts. The cysts in this study had a membrane-like surface over a smooth scale-like inner layer. Furthermore, a plug -like closure was seen in one of the intact cysts; a statospore-like empty cyst also was observed. Cyst formation could be the way to survive in temperate areas such as Dutch coastal waters, where winter temperatures are lethal for vegetative cells.

Introduction

The marine raphidophyte microalga *Fibrocapsa japonica* is a yellow-brown to golden-brown naked flagellate of 25–40 µm long and 15–20 µm wide (Hara and Chihara, 1985). Blooms of *F. japonica* are known to be associated with massive fish mortality events (Iwasaki, 1971; Okaichi, 1972; Toriumi and Takano, 1973). During the past decades, *F. japonica* has been observed world-wide. An anthropogenically aided distribution has been suggested because of the lack of genotypic variation between strains isolated worldwide and the presence of lethal temperature boundaries between their habitats (Kooistra *et al.,* 2001; de Boer *et al.,* 2002). *F. japonica* in Dutch coastal waters may survive cold winters or may be transported in ballast water of ships due to cyst formation enabling (re)inoculation under favorable conditions.

Information on the life cycle of *F. japonica* is limited; a cyst stage was reported only once in field samples using light microscopy (Yoshimatsu, 1987). These cysts were spherical, 15–20 µm in diameter, brownish, and the cell wall was smooth (Yoshimatsu, 1987). The cysts were present in sediment from the Seto Inland Sea, Japan, and were frequently observed adhered to diatom frustules (Yoshimatsu, 1987). Cysts of *F. japonica* may produce extracellular products that attach them to frustules (Imai, 1989). After germination, an empty cyst remains (Yoshimatsu, 1987).

Until now, cysts of *F. japonica* were never observed under laboratory conditions. For other raphidophytes, such as *Chattonella* sp., storage temperatures at or below 11°C for over 4 months were needed for maturation of cysts under laboratory conditions (Imai, 1990). Also, a combination of factors was effective for cyst formation in *Chattonella* sp.: nutrient depletion (especially N limitation), adherence to solid surfaces (glass beads or glass slides), and a low irradiance (darkness–15 µmol photons · m^{-2} · s^{-1}) (Imai, 1989; 1990; Nakamura and Umemori, 1991). In this laboratory study, a similar procedure was used to induce cyst formation of *F. japonica* using strains recently isolated from Dutch coastal waters.

Methods and Observations

Strains Md0913i and Md0913iii genetically identified as *Fibrocapsa japonica* (Kooistra *et al.,* 2001) and originating from the Marsdiep, Dutch Wadden Sea, were used. Both strains were not axenic and pre-cultured in f/2 enriched seawater (Guillard, 1975). Cultures were maintained at 17°C ± 1°C, under 16:8 h Light/Dark cycle, at a salinity of 25 practical salinity units (p.s.u.) and a photon flux density of 35 ± 5 µmol photons · m^{-2} · s^{-1}. After a period of exponential growth, batch cultures reached their stationary phase due to nutrient depletion; the cultures had a cell density of at least 10^5 cells · mL^{-1}. Five duplicates of the pre-cultured strains, 2 of Md0913i and 3 of Md0913iii were used for cyst formation. Each culture received 3 cover slides (17.5 × 17.5 mm), glued to 30 cm long cotton threads for easy removal, on the bottom of the flasks for enabling attachment of cysts. Before use, the slides were cleaned with ethanol. Each culture was acclimated for 2 days at 16°C ± 0.5°C on half the amount of light (±20 µmol photons · m^{-2} · s^{-1}), followed for 5 days at 12°C ± 0.1°C at dim light conditions (<10 µmol photons · m^{-2} · s^{-1}). After this incubation period, one culture of the duplicates was placed in the dark at 12°C and the other at 5.5 ± 0.2°C.

After 9 months of incubation, most slides were covered with a brownish biofilm. These slides were used for cyst observations. For cryoSEM, the biofilm was put on a grid, frozen in N-slush at –210°C, and placed on a stub. The stubs with biofilm were transferred in an Oxford (UK) CT 1500 HF high-resolution cryotransfer system for SEM, etched at –95°C for 5 minutes, coated with 3 nm gold/palladium and examined at –120°C in a Cryo-FEG-SEM, type: Jeol JSM-6301F. Slides of cultures incubated at 5.5°C and 12°C were analyzed, but no cells or cysts were found. However, an evenly distributed polymer network was observed (Fig. 1A).

Light microscopic observations of cover slides were negative at 12°C, but at 5.5°C some cysts were seen. These cysts were spherical and dark brown as described before (Yoshimatsu, 1987).

Steidinger, K. A., J. H. Landsberg, C. R. Tomas, and G. A. Vargo (Eds.). 2004. Harmful Algae 2002. Florida Fish and Wildlife Conservation Commission, Florida Institute of Oceanography, and Intergovernmental Oceanographic Commission of UNESCO.

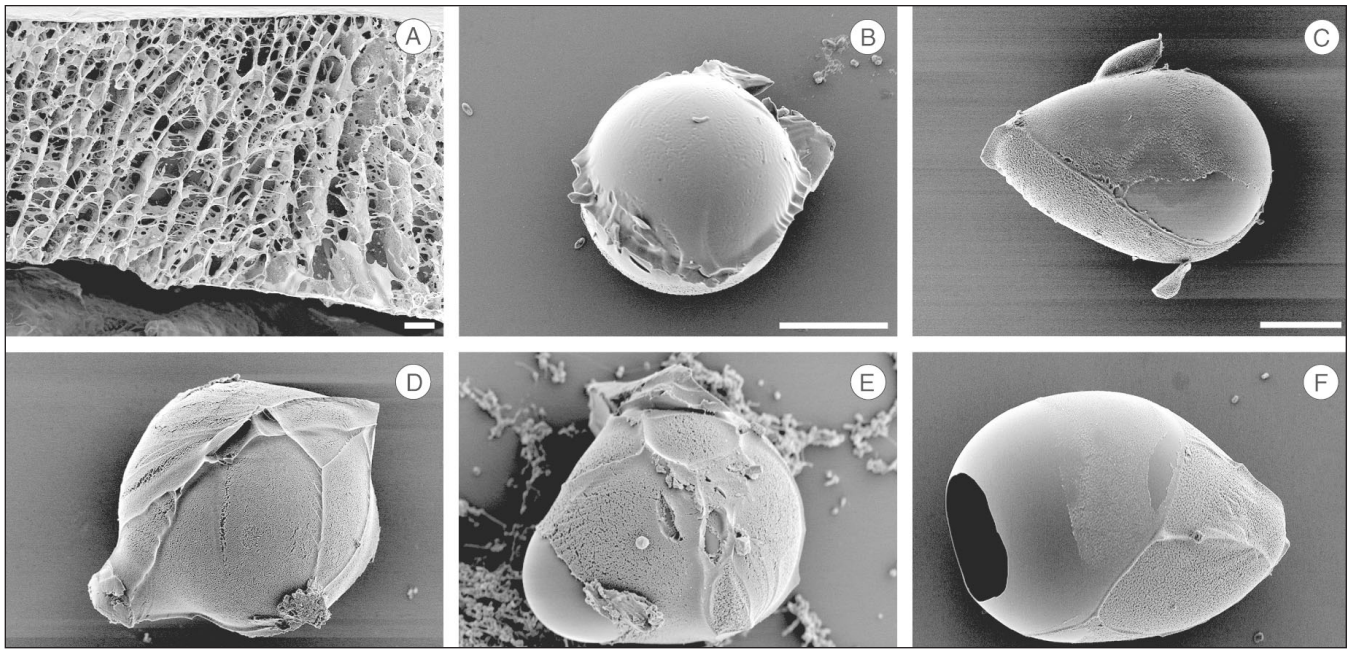

Figure 1 Scanning Electron Micrographs of **A** a fractured cross-section of a biofilm from the cover slides that were submerged in batch cultures incubated for nine months in the dark, and of *Fibrocapsa japonica* cysts **B**–**E** and a statospore-like empty cyst **F**; bar length 10 μm.

To reveal cysts embedded in the network seen with the cryoSEM method, we fixed biofilms for 24 h in 2% glutaraldehyde (0.2 M cacodylate buffer). After fixation, these biofilms were critical-point dried, mounted on stubs, coated with 3 nm gold/palladium, and examined at 20°C with a FEG-SEM, type: Jeol JSM-6301F. On the slides from the 5.5°C strain Md0913i, cysts were observed (Figs. 1B–E) and one statospore-like empty cyst was found (Fig. 1F), but no cysts were found in the biofilms from the 12°C cultures.

Discussion

Cysts of *F. japonica* were formed in the cultures that were kept at 5.5°C in the dark. The density of *F. japonica* cysts on the slides was very low despite the use of high density cultures, and a combination of nutrient limitation, darkness and low temperatures. The number of our observations was too limited to conclude that the lack of cysts at 12°C was due to higher temperatures. Each cyst seemed to have a membrane-like surface over a smooth scale-like inner layer (Figs. 1C, E, F). The empty cyst (Fig. 1F) resembled the statospore cysts of the Chrysophyceans. This class, closely related to the Raphidophyceae, has characteristic statospores also known as stomatocysts or siliceous cysts, where the wall is pierced by a pore, stoppered by a plug of polysaccharide (van den Hoek *et al.,* 1995; Graham and Wilcox, 2000). Similar structures were observed for two other raphidophytes: *Olisthodiscus luteus* (Hara *et al.,* 1985) and *Chattonella* sp. (Imai, 1990), but not for *Heterosigma akashiwo* (Han *et al.,* 2002). Statospore-like empty cysts of *O. luteus* have a thick wall and a circular opening without any appendages such as a collar and spine-like protrusions (Hara *et al.,* 1985). The same morphology was observed for empty cysts of *Chattonella* sp. but next to the opening a lid was visible, suggesting that opening is a particular structure for germination (Imai, 1990). Not a lid, but rather a plug-like closure was seen in one of the intact *F. japonica* cysts (Fig. 1E). So far, the chemical composition of the membrane-like surface, the smooth scale-like inner layer and the plug of *F. japonica* cysts remains unknown.

Unfortunately, the biofilm on the cover slides was too thick (>80 μm) to observe *F. japonica* cysts from above with the cryoSEM method. No cysts were found in the network either, after the frozen biofilm was fractured and a small section of the network was investigated. The smooth, even network on the slides could be composed of the ejected mucus from dying *F. japonica* cells, sticking the cysts of *F. japonica* to the slides. Production by bacteria, however, also could be responsible for this network. *H. akashiwo* cells excrete copious amounts of mucus surrounding the resting cells (Imai *et al.,* 1993), encapsulate the non-motile cells (Tomas, 1978), and form pelagic filaments during blooms (Pratt, 1966). Besides a possible attachment function, an external polysaccharide matrix would protect the wall-less raphidophytes from disruption in the benthic sediment (Han *et al.,* 2002).

The size and form of *F. japonica* cysts formed under laboratory conditions seem to be similar to their natural cysts (Yoshimatsu, 1987). Experiments with natural cysts have indicated that *F. japonica* and *Chattonella* sp. cells require a period of dormancy of at least a few months (Yoshimatsu, 1987; Imai, 1990). Here we have shown that after a period of 9 months, *F. japonica* cysts are still intact, although the viability is unknown. The ploidy of *F. japonica* cysts also remains unknown.

In the Wadden Sea and the southern North Sea, vegetative cells were observed only in summer. In the laboratory, the vegetative cells did not survive a period of 16 days below 4°C (unpublished results). Presumably *F. japonica* spends part of its life cycle as cysts in the sediment. Formation and viability of cysts for at least several months may well be the only way to survive the cold winter period; alternatively, cysts may be (re)inoculated in the Dutch coastal zone from elsewhere.

Acknowledgements

M. K. de Boer was supported financially by NWO-ALW project 809.34.004, M. van Rijssel by the NWO Prioriteit Programme "Sustainable use and conservation of marine living resources," theme 3. We wish to thank Jan Zagers, Itze Stokroos and Monika R. Tyl for their assistance with SEM. We are grateful to Reinoud P. T. Koeman for isolation of the *F. japonica* strains. We acknowledge Dick Visser for graphics and W. W. C. Gieskes, B. Dale and an unknown reviewer for editorial advice.

References

M. K. de Boer, E. M. Koolmees, W. W. C. Gieskes, E. G. Vrieling, A. M. Breeman and M. van Rijssel, this Proceedings.

L. E. Graham and L. W. Wilcox, Algae (Prentice-Hall, Inc., Upper Saddle River), pp. 1–640 (2000).

R. R. L. Guillard, in: Culture of Marine Invertebrate Animals, W. L. Smith and M. H. Chanley, eds. (Plenum Press, New York), pp. 108–132 (1975).

M. S. Han, Y. P. Kim and R. A. Cattolico, J. Phycol. 38, 304–317 (2002).

Y. Hara and M. Chihara, Arch. Protistenk. 130, 133–141 (1985).

Y. Hara, I. Inouye and M. Chihara, Bot. Mag. Tokyo 98, 251–262 (1985).

C. van den Hoek, D. G. Mann and H. M. Jahns, Algae, an Introduction to Phycology (Cambridge University Press, Cambridge), pp. 1–627 (1995).

I. Imai, Mar. Biol. 103, 235–239 (1989).

I. Imai, Bull. Nansei Natl. Fish. Res. Inst. 23, 63–166 (1990).

I. Imai, S. Itakura and K. Itoh, Nippon Suisan Gakkaishi 59, 1669–1673 (1993).

H. Iwasaki, J. Oceanogr. Soc. Jpn. 27, 152–157 (1971).

W. H. C. F. Kooistra, M. K. de Boer, E. G. Vrieling, L. B. Connell and W. W. C. Gieskes, J. Sea Res. 46, 213–222 (2001).

A. Nakamura and T. Umemori, Mar. Ecol. Prog. Ser. 78, 273–284 (1991).

T. Okaichi, in: The Cause of Red Tide in Neritic Waters, Anon., eds. (Japanese Association for the Protection of Fisheries Resources, Tokyo), pp. 58–76 (1972).

D. M. Pratt, Limnol. Oceanogr. 11, 447–455 (1966).

C. R. Tomas, J. Phycol. 14, 314–319 (1978).

S. Toriumi and H. Takano, Bull. Tokai Reg. Fish. Res. Lab. 25–35 (1973).

S. Yoshimatsu, Bull. Plankton Soc. Jpn. 34, 25–31 (1987).